# Synthesis and Photophysical Properties of Gold(III) and Pt(II) Complexes bearing Persistent Radicals

**Master of Research**

**by**

**SANDHYA VERMA**

**45037396**

**Faculty of Science and Engineering**

**Department of Molecular Sciences**

**Supervisor**

**Assoc. Prof. Koushik Venkatesan**

**Macquarie University**

**April 2019**

## Acknowledgments

I would like to thank Dr. Koushik Venkatesan for offering me this opportunity to study here in Australia and introducing me to the world of organometallic chemistry. Koushik gave his consistent support and supervision throughout the duration of my MRes study.

I would like to thank my group members Robert, Dominik, Tobias, Teja for constantly encouraging me during my whole project. All the group members were humble and created a great atmosphere in and around the lab. I am grateful to Robert for his patient guidance during my research work.

Macquarie University and whole MRes Committee for providing enthusiatic research environment. I am also thankful to iMQRTEP Fellowship for providing funds.

Dr. Matthew Mackay and his student Matthew Fitzhenry for HR-ESI-MS measurements and analysis by mass spectrometry at Macquarie University.

Remi Rouquette for elemental analysis at Macquarie University.

Dr. Nick Cox and his student Julien Langley for EPR measurements and analysis of the results at Australian National University, Canberra.

My Parents for supporting me throughout my education.

My Husband for his immense love and trust.

## Statement of the Candidate

I Sandhya Verma hereby declare that the presented work in the thesis is my original research work. Wherever contributions of others are involved, every effort is made to indicate this clearly, with due reference to the literature, and acknowledgement of collaborative research and discussions. This work was done under the guidance of Assoc. Prof. Koushik Venkatesan at Macquarie University, Sydney, Australia.

**SANDHYA VERMA**

In my capacity as supervisor of the candidate's thesis, I certify that the above statements are true to the best of my knowledge.

**KOUSHIK VENKATESAN**

# Abstract

Organic Light Emitting Diodes (OLEDs) represent the next generation lighting technology. Transition metal complexes that exhibit luminescent properties have been investigated as triplet emitters for applications in OLED devices. Metal complexes bearing a persistent radical offer an interesting avenue to tune the excited-state properties, which could provide alternative emitter systems that has been only scarcely investigated. Presence of coordination sites at the radical ligands allows the metal centres to be coordinated, which is expected to modulate the photophysical and photochemical properties such as luminescence quantum yield, emission wavelength maxima and the stability in the photoexcited state. The organic radicals 2-(4-ethynylphenyl)-4,4,5,5-tetramethylimidazolidine-1,3-diol (nitronyl nitroxide) and (3,5-dichloro-4-pyridyl)bis(2,4,6-trichlorophenyl)-methyl (PyBTM) were chosen as ligands due to their photo- and thermal stability. The present work reports the synthesis, characterization and detailed photophysical investigations of new cyclometalated Au(III) and Pt(II) complexes bearing nitronyl nitroxide and PyBTM as ligands, respectively. The resulting final complexes were stable to air and moisture. The photophysical investigations are strongly suggestive of an interplay between the radical spin and the triplet excited state. The outcomes of the thesis are expected to lead to an efficient strategy for altering the excited state properties of luminescent materials which could be applied for achieving efficient light emitting devices.

# Table of Contents

# 1. Introduction and Background

## 1.1 Photoluminescence

When sample is irradiated with light, absorption of photons occurs which affords excess energy to the material and this process is termed as photoexcitation. The dissipation of this excess energy by the sample through emission of light is known as luminescence. This type of luminescence is termed as photoluminescence as it is a result of photoexcitation. Because of photoexcitation electrons within the material move into permissible excited states. Excess energy is released when these electrons return to their equilibrium states and this process causes the emission of light (a radiative process) or may not result in any emission (a non-radiative process). The difference in the energy levels among the two electronic states involved in the transition between the excited state and the equilibrium state corresponds to the energy of the emitted light (photoluminescence). The quantity of the emitted light is related to the comparative contribution of the radiative process.[1]

## 1.2 Jablonski Diagram

When irradiated with light, electron in the singlet ground state ($S_0$) absorbs energy and gets promoted to the excited singlet state ($S_n$). From there it has various possibilities to return to the ground state figure 1. Fluorescence occurs when the electron in the excited state returns to the ground state by emitting light without changing (or flipping) its spin multiplicity. It is the most common radiative short lived photophysical process. The movement of electrons from the higher vibrational states to the lower vibrational states without changing its spin multiplicity is termed as internal conversion (IC). It is the fastest non-radiative process. When the electron in the singlet excited state moves to the triplet excited state via changing its spin multiplicity, it is known as intersystem crossing (ISC), which is a non-radiative process. When electron in the excited triplet state ($T_n$) returns to the singlet ground state ($S_0$) through a radiative process the phenomenon is termed as phosphorescence.

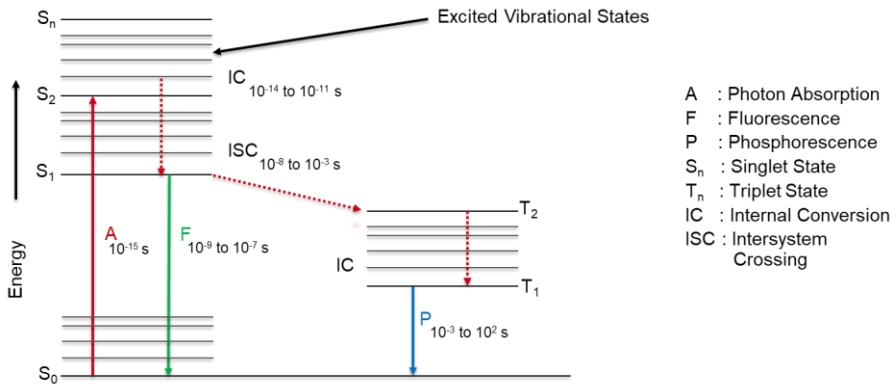


**Figure 1.** Energy Level Diagram - Jablonski Diagram.

Absorption of photons in the form of energy by an electron in the singlet ground state gets promoted to the singlet excited state, the deactivation of this electron back to singlet ground state results in fluorescence. The electronic spin is conserved with respect to the ground state. When the electron in the excited state returns to the ground state, emission of a photon of lower energy takes place, which corresponds to a longer wavelength than that of the absorbed photon (Stokes shift). The phenomenon of fluorescence has a short lifetime ($10^{-8}$ to $10^{-4}$ s). The dashed arrows represent a non-radiative processes.

## 1.3 Potential Energy Curve for Fluorescence and Phosphorescence

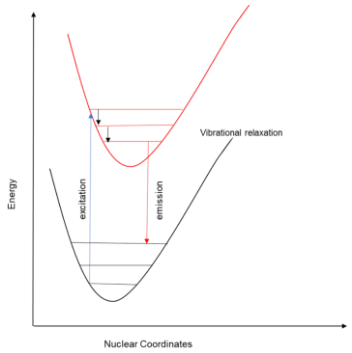


**Figure 2.** Potential energy curve showing fluorescence.

The electron in the excited state might simply return immediately and photon would be emitted of the same wavelength as that of the absorbed photon. Conversely, if the electron relaxes into a lower vibrational level, a part of its initial energy is lost as heat as shown in figure 2. This relaxation of this electron back to the ground state leads to fluorescence. Usually fluorescence occurs in molecules having a degree of conjugation. The intensity of the emission is determined by the molecular structure and chemical environment.

Phosphorescence is a radiative process, in which the electron in the singlet excited state undergoes intersystem crossing into a triplet excited state with a reversed spin multiplicity as shown in figure 3.

The lifetime of phosphorescence is much longer than that of fluorescence usually from$10^{-4}$ - $10^{-2}$ s. Thus, unlike fluorescence, emission of light does not take place faster in the case of phosphorescence. Therefore, phosphorescence is even more rare than fluorescence, since a molecule in the triplet state can easily undergo intersystem crossing to ground state before phosphorescence can occur.

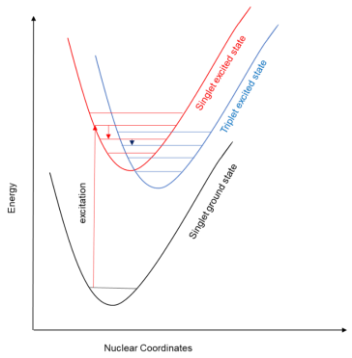


**Figure 3.** Potential energy curve showing phosphorescence.

## 1.4 Luminescent Organic Radicals

For a long time stable organic radicals were considered as non-emissive or highly light-sensitive species[2]. Unique emission characteristics of stable organic radicals have been revealed recently, based on their doublet states ($D_0$), an effective electron-photon conversion in electroluminescent devices in the absence of the heavy metal effect. The major problem which hinders investigating photofunctions of luminescent organic radicals is the molecular degradation upon photoexcitation.[3–6] Developing methods to enhance the photostability of luminescent organic radicals to enlarge their scope to have an interplay between the luminescent, magnetic, and electronic properties is expected to provide magnetic (spin), electronic, and photo responsive molecular devices.[2]

Luminescent organic molecules are fascinating since they are suitable for various applications such as OLEDs and chemosensors. To obtain the desired device properties several emission mechanisms have been used such as fluorescence via the singlet excited state, phosphorescence via triplet excited state and thermally activated delayed fluorescence.[7]

The nature of the excited states of a luminescent molecule strictly determines the emissive behaviour.[8] The luminescence properties exhibited by radicals having an unpaired electron from the doublet excited state ($D_1$) to the doublet ground state ($D_0$) displays unique characteristics such as long emission wavelength and high efficiency in electroluminescent devices without extended $\pi$-conjugation.[9,10] This spin allowed transition without quenching *via* ISC produces high internal quantum efficiency in electroluminescent devices.[11]

### 1.4.1 Open Shell Organic Radicals

The open shell electronic structures of organic radicals have various unusual properties and can be useful to applications in various fields such as spintronics, molecular magnets, electron paramagnetic resonance (EPR) imaging, organic field-effect transistors (OFETs), organic rechargeable batteries and accelerating chemical reactions.[12–16]

Harvesting the triplet excited state from traditional organic closed shell molecules has always been challenging because of the spin forbidden transition of the triplet exciton to the ground state.[17] Thermally activated delayed fluorescence (TADF), triplet-triplet annihilation (TTA) processes are supposed to resolve the problem of triplet harvesting.[18,19] In contrast, since radicals display doublet emission, the occurrence of spin allowed transition of doublet excitons to the ground state resolves the problem of harvesting triplet energy in OLEDs.[20]

Significant quenching of fluorescence occurs when open-shell radical species are introduced into luminescent closed shell molecules.[6] Whereas quenching does not occur in monoradicals where triplet state ($T_1$) is generated statistically together with the lowest singlet excited state (S1) in a ratio of 3:1 due to the absence of excited states between $D_1$ and $D_0$ and spin-allowed $D_1$-$D_0$ transition.[2]

### 1.4.2 PyBTM as Stable Luminescent Organic Radical

A fluorescent organic stable radical perchlorotriphenyl methyl radical (PTM) with $\lambda_{em}$= 605 nm and $\Phi$ = 0.015 in $CCl_4$ is chemically stable under ambient conditions but decomposes when irradiated with light into a non-fluorescent perchloro-9-phenylfluorenyl radical which has a quantum efficiency of 0.3.[21,22] To overcome this problem of degradation Nishihara et. al developed a novel PyBTM (3,5-dichloro-4-pyridyl)bis(2,4,6-trichloro-phenyl)methyl radical with a unique molecular design and found to have excellent stability under ambient conditions and photoirradiation.[20]

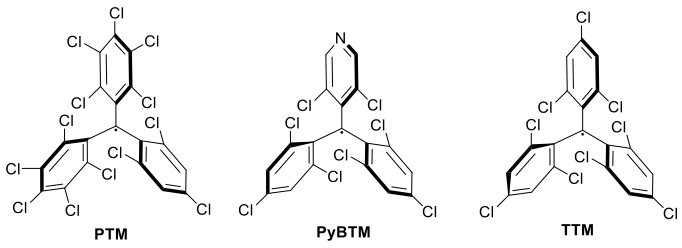


**Figure 4.** Structure of PTM, PyBTM, TTM.

It was supposed that incorporation of pyridine ring into the TTM skeleton would lower the energies of frontier molecular orbitals on the TTM skeleton because of greater effective nuclear charge (electronegativity) of the nitrogen atom as compared to the carbon atom which results in enhanced photostability.[4] On excitation at $\lambda$= 370 nm, the fluorescence spectra of PyBTM in $CH_2Cl_2$ showed

an emission band at maxima $\lambda$ = 585 nm. To support the fact that the emission is fluorescent in nature the observed excited state lifetime of this radical is 6.4 ± 0.2 ns in dichloromethane which is comparable to those of TTM ($\tau$= 7.0 ± 0.2) ns and PTM ($\tau$ = 7 ns). The rationalised photophysical process of PyBTM can be summarised as follows: The photoexcitation of radical with light at $\lambda$ = 370 nm induces electronic transition primarily 129$\alpha$→130$\alpha$ and 129$\alpha$→131$\alpha$ centred on the $\alpha$ spins thus resulting in the formation of D$\alpha_1$ and D$\alpha_2$ excited states. The deactivation of these excited states to the lowest excited state D$\beta_1$($D_1$) is represented by the $\beta$-spin excitation (128$\alpha$→129$\beta$). The emission process of conventional closed-shell molecules does not hold such rearrangement of excited spin states. The spin allowed nature of the photophysical processes of this radical follows Kasha's rule. Finally, the relaxation of $D_{\beta 1}$ to $D_0$ takes place with a fluorescence emission.

PyBTM radical has shown excellent luminescent properties at 77 K and an absolute photoluminescence quantum yield of 0.81 in EPA (diethylether:isopentane:ethanol 5:5:2) which is the highest of the values reported for stable organic radicals. The quantum yield of the system is ten times enhanced in comparison to the solution when PyBTM radical is encapsulated in PMMA matrix. The stability of PyBTM towards light is enhanced up to 115 times higher than that of the tris(2,4,6-trichlorophenyl)methyl (TTM) radical. Protonation of PyBTM by the addition of acid significantly affects the luminescence and redox properties, thereby demonstrating the drastic change in the electron-accepting ability of the molecule upon protonation. The electronic and optical properties of the radical by protonation and deprotonation is controlled actively through the introduction of pyridine ring which acts as a proton coordination site.

Photostability is an important problem for luminescent radicals.[23] On a way to enhance the photostability of the luminescent triaryl methyl radicals introducing an additional pyridyl ring to the PyBTM skeleton is considered beneficial as increase in number of pyridyl ring would expand the variation of the coordination sites thereby resulting in the formation of various dimensional assemblies[24–26]. To study the effect of introducing an extra pyridyl group bis(3,5- dichloro-4-pyridyl)(2,4,6-trichloro-phenyl)methyl radical bisPyTM was synthesized which is stable and luminescent.[27]

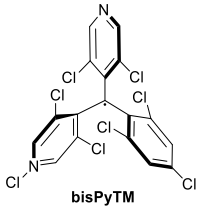

bisPyTM

**Figure 5.** Structure of bisPyTM

Solution of bisPyTM in dichloromethane displayed fluorescence with emission wavelength $\lambda_{em}$ of 650 nm when excited with $\lambda_{ex}$ = 355 nm. The structural change of bisPyTM in the excited state causes a strong red-shift in the emission wavelength. The observed excited state lifetime and fluorescence quantum yield is 3.6 ns and 0.009 respectively. Luminescence properties of bisPyTM is well exhibited in solution as well as in crystalline state.[28] Emission wavelength of 712 nm was observed for crystalline state of bisPyTM. Doping concentration of 3.0 wt% bisPyTM into its precursor, $\alpha$H-bisPyTM crystal shifts the emission wavelength to the shorter wavelength which is due to the decrease in reorientation energy caused by rigid packing. With the increased doping concentration, the emission wavelength was red shifted and the intensity was decreased suggesting the excimer formation. The observed half-life ($t_{1/2}$) value of bisPyTM in dichloromethane was 6.7 X $10^3$ s which is 43 times larger than PyBTM.[23]

### 1.4.3 Radical based Organometallic Complexes

To enhance the luminescent properties of PyBTM radical it is coordinated with Au(I) as metal centre because it can coordinate well with pyridine and its derivative with gold complexes are known to show excellent luminescence properties.[29–31] Photophysical and photochemical properties were studied for the synthesized [Au(PyBTM)$PPh_3$]$ClO_4$ and [Au(PyBTM)$PPh_3$]$BF_4$.[32,33]

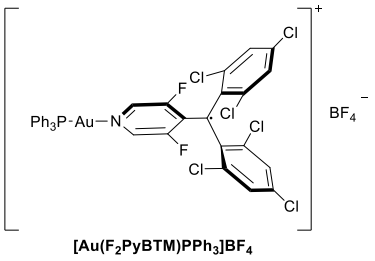

[Au($F_2$PyBTM)$PPh_3$]$BF_4$

**Figure 6.** Structure of [Au($F_2$PyBTM)$PPh_3$]$BF_4$

Characteristic transition bands were observed for this radical gold complex at $\lambda_{abs}$= 566, 434 and 380 nm in UV/Vis absorption spectrum. The DFT calculations revealed that excitation of the transition band is due to $206\beta \rightarrow 207\beta$ transitions which generate $D_1$ state and results in fluorescence. The absolute photoluminescence quantum yield for this complex was 8% which was four times than that of PyBTM (2%). The observed fluorescence lifetime $\tau$ of 13.1 ± 0.2 ns was twice than that of PyBTM (6.4 ± 0.2 ns). The coordination of Au(I) also enhanced the photostability with an estimated half-life ($t_{1/2}$) of (5.0 ± 1.1) X $10^4$ s which is thrice that of PyBTM(1.5 ± 0.2) X $10^4$ s.

To further enhance the fluorescence quantum yield of the [Au(PyBTM)$PPh_3$] $BF_4$ complex, one of the approaches is to introduce fluorine on the pyridine ring as electron withdrawing nature of the fluorine lowers the energy of the β-NHOMO more than β-SOMO to result in a larger energy gap

between $D_1$- $D_0$. This is because the angle between the pyridyl ring and the plane of $sp^2$ hybridized central carbon (=$\theta$) would decrease due to fluorine substitution, because of smaller Van der Waals radius of a fluorine atom than that of a chlorine atom. Consequently, $\pi$-conjugation between the two moieties is expected to enhance in fluorine-substituted radicals, which certainly is the reason of higher quantum yield. Indeed, $\theta$ was smaller in $F_2$PyBTM (33.31°) than in PyBTM (49.31°) in their crystal structures, suggesting the possibility to form stronger $\pi$-conjugation in the fluorine-containing radicals in solution.

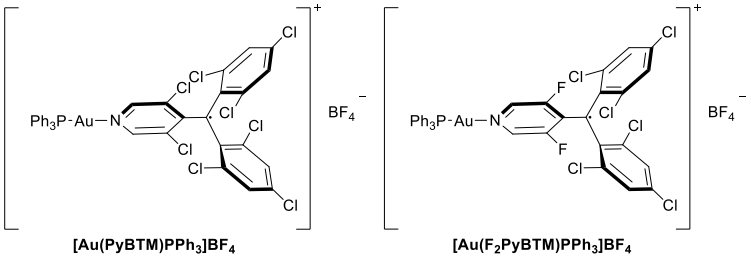


**Figure 7.** Structures of [Au(PyBTM)$PPh_3$]$BF_4$ and [Au($F_2$PyBTM)$PPh_3$]$BF_4$.

The hypsochromic shifts of [Au($F_2$PyBTM)$PPh_3$]$BF_4$ relative to [Au(PyBTM)$PPh_3$]$BF_4$ confirms the large energy gap which further results in smaller Frank-Condon factors, displaying slower internal conversion thus resulting in lower $k_{nr}$. [$Au^1$($F_2$PyBTM)$PPh_3$]$BF_4$ displayed an absolute quantum yield of 20% and fluorescence lifetime of 35.7 ns in dichloromethane, while quantum yield of [Au(PyBTM)$PPh_3$] $BF_4$ was 8% and fluorescence lifetime of 13.2 ns which is higher than that of PyBTM radical.

Another paramagnetic, organometallic gold(I) complex Au($C_6F_5$) (PyBTM) was reported to have interesting luminescent properties. Density functional theory and time-dependent (TD)-DFT calculations indicated that the fluorescence occurring in $CCl_4$ is due to interligand charge transfer (CT) where $C_6F_5$ and PyBTM moieties operate as electron donor and acceptor respectively. [24,27]

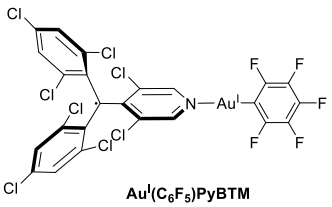


**Figure 8.** Structure of Au($C_6H_5$)PyBTM.

This gold(I) radical complex displayed an emission at $\lambda_{em}$ = 619 nm when excited with $\lambda_{exc}$ = 416 nm upon photoirradiation in $CHCl_3$ and resulted in $\Phi_{em}$ = 0.04 and emission lifetime ($\tau$) of 7.1 ns signifying its fluorescence character. When compared with the second transition band of PyBTM

which is visibly shifted towards the red in the lower energy region 550-600 nm, suggesting PyBTM centred photoexcitation process. It can be summarised that substitution of fluorine and coordination with gold(I) interactively affect the electronic excited states of the radical thereby increasing the quantum yield and causing shifts in absorption and emission wavelengths. When dissolved in different halogenated solvents complex Au($C_6F_5$)(PyBTM) displayed unique luminescent properties. Solvents like $CCl_4$, $CHCl_3$, $CH_2Cl_2$, and $ClCH_2CH_2Cl$ affects the luminescence characteristics of radical gold(I) complex. It was observed that fluorescence quantum yield ($\Phi_{em}$) enhances and emission wavelength ($\lambda_{em}$) is lowered when the polarity (dielectric constant) of the solvent is decreased. $\lambda_{em}$ shifted to the long wavelength region as the polarity of the solvent increased. Since it was observed that luminescent molecules typically emit from CT excited state it can be concluded that the molecules are more polar in excited state ($D_1$ state) than in the ground state ($D_0$ state).

Highest reported fluorescence quantum yield of PyBTM derivative is 23% in $CCl_4$[8]. Fluorescence lifetime of Au($C_6F_5$)(PyBTM) in $CCl_4$ and $CHCl_3$ displayed single emissive component with $\tau$ = 32 and 7.1 ns, respectively where as $CH_2Cl_2$ and $ClCH_2CH_2Cl$ had two emissive components which was revealed at around 635 nm with a smaller shoulder at 580 nm. Consequently, solvent dependent fluorescence was observed for the first time in radicals.[34,35]

### 1.4.4 Magnetic Properties in Luminescence Organic Radicals

Free radicals exhibit paramagnetic behaviour as they contain unpaired electrons and have magnetic moments that are attracted to the magnetic field. Electronic behaviour in an organic molecule can be modulated via applying external magnetic field. It is also useful in investigating the fundamental molecular properties. Change in electrical resistance caused due to magnetic field is termed as magnetoresistance and is used industrially in reading and writing memory hard drives.[36]

Modulation of magnetic field greatly affects the rate of intersystem crossing in the luminophores having excited states with different spin multiplicities.[37–40] Distribution of spin states (i.e., spin statistics) in the excited state is altered with the modulating magnetic field which further results in the species possessing magnetic field sensitive luminescent properties.[41,42] Magnetic field substantially effects the processes such as triplet-triplet annihilation which involves changes in the spin multiplicity of the excited state.[43] Magnetoluminescence is a new term introduced to understand the interplay between luminescence and magnetic spin to develop new photofunctionalities.[36] Magnetic field sensitive emission properties are shown by PyBTM radical when doped into *aH*-PyBTM host crystals.

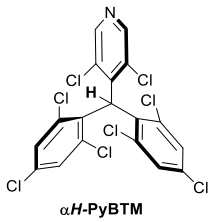


**Figure 9.** Structure of α*H*-PyBTM

Random dispersion of PyBTM radical in host crystal causes aggregation and produce spin states with different multiplicities in the excited state which displays magnetic-field-sensitive emission properties which are different from the isolated PyBTM in a doublet state. The luminescence displayed by 0.05 wt% doped crystals exhibited remarkably high quantum yield ($\Phi_{em}$) of 89% under ambient conditions. Increased doping concentration results in a broad emission band at $\lambda_{em}$ = 680 nm which is attributed to the excimer formation.[44,45] Doping with 10 wt% of radical in host crystal exhibits magnetoluminescence at 4.2 K which is suggestive that the excimer emission occurring does not necessarily come from radical pair (dimer) rather it is from other oligomeric species, such as trimer.

### 1.4.5 Heavy Metal Effect on Luminescent Radicals

Luminescence properties of stable radicals are significantly affected by a heavy atom as they tend to accelerate the intersystem crossing and helps in quenching fluorophore emission of closed shell molecules.[5] These radicals have enough coordination sites for heavy metal ions which further can enhance the luminescence properties.[24,46–48] Nishihara et.al synthesised [2-chloro-6-(2-pyridyl)-3-pyridyl]bis(2,4,6-trichlorophenyl)methyl radical (oPyPyBTM') and [2-chloro-6-(4'-2,2':6',2''-terpyridyl)-3-pyridyl]bis(2,4,6-trichlorophenyl)methyl radical (tpyPyBTM') to investigate the coordination of pyridyl or terpyridyl with cations including protons, fourth period metal ions and lanthanide ions.

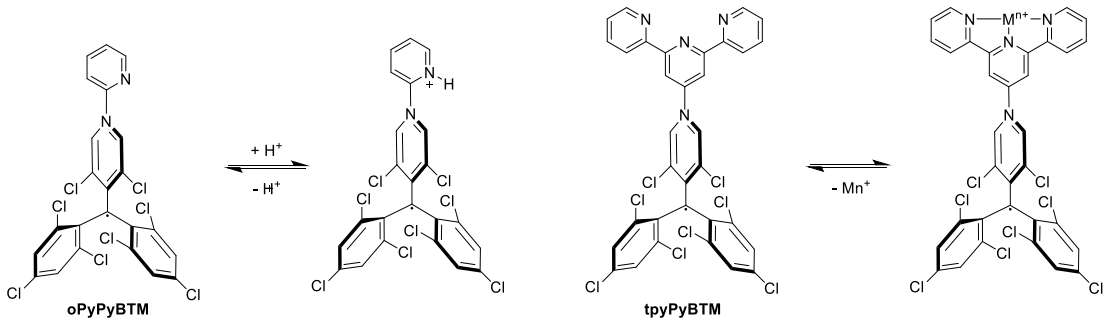


**Figure 10.** Structures showing protonation on oPyPyBTM and metal coordination on tpyPyBTM.

Turn on fluorescence was observed when protonation of the pyridyl ring occurred. Coordination of tridentate motif of tpyPyBTM with metal ions such as $Zn^{2+}$ also reveals turn on fluorescence and resulted in $\Phi$ = 3.0%. While coordination with other metals ions such as $Cu^{2+}$, $Ni^{2+}$, $Fe^{2+}$, and $Mn^{2+}$ suppressed the fluorescence because of energy or electron transfer. Addition of $La^{3+}$ to tpyPyBTM increased fluorescence and the quantum yield $\Phi$ = 4.1% signifying that there is no heavy atom effect.

### 1.4.6 PyBTM Radical bearing Carbazole Moiety

TTM-1Cz(4-N-carbazolyl-2,6-dichlorophenyl)bis(2,4,6-trichlorophenyl)methyl is a known emitter for OLEDs. For a molecule to be deposited over thin films, its stability under high vacuum is the major criteria. TTM-1Cz remains chemically stable even after heating under high vacuum which is proved by EPR and NMR spectra of the deposited sample.[49] When fabricated with conventional fluorescent material NPB (N,N'-di-1-naphthyl-N,N'-diphenylbenzidine) and CBP(4,4-bis(carbazol-9-yl)biphenyl) into a thin film of ITO/NPB (30 nm)/CBP (10 nm)/TTM-1Cz:CBP (5wt%, 40 nm)/TPBi (35 nm)/LiF (0.8 nm)/Aluminium (100 nm) it shows blue emission of NPB and red emission of TTM-1Cz. Magento-electroluminescence (MEL) was observed for the NPB layer suggesting the presence of triplet excitons whereas no MEL was detected for TTM-1Cz which clearly proves the absence of triplet exciton in the TTM-1Cz thus emission in OLED is due to doublet.[50–54]

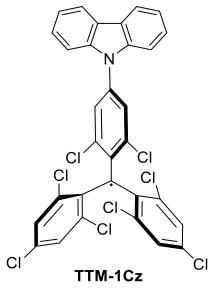


**Figure 11.** Structure of TTM-1Cz

The maximum external quantum efficiency achieved by the OLED device made of TTM-1Cz is 2.4%, which is comparable to those of deep-red/near-infrared OLEDs. With the expanding field of organic photoluminescent radicals a lot has been done on PyBTM radical in a very short period. Due to its interesting photophysical properties it is a promising candidate for introduction of this radical into a luminescent molecular scaffold. This provides a wide scope of possibilities to enhance photophysical properties of luminescent materials which could be useful for a number of light emitting applications.

## 1.5 Fluorescent Dithiadiazolyl Radical

Polyaromatic hydrocarbons incorporated with electron donating or withdrawing substituents can contribute to control the supramolecular arrangements in molecules in the condensed phase to ensure better performance of light emitting devices. [55–59] Stable thiazyl radicals are used as building blocks in material chemistry as they exhibit high conductivities. Additionally, they are used as organic magnets and as paramagnetic ligands. [60] Combination of stable thiazyl radicals with polyaromatic hydrocarbons (PAHs) widely opens possibilities of developing advanced functional materials.

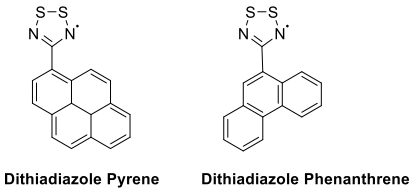


**Figure 12**. Structure of Pyrene and Phenanthrene based Dithiadiazolyl radicals.

The optical properties of dithiadiazolyl pyrene and dithiadiazolyl pyrene [$GaCl_4$**]** in acetonitrile revealed the emissive behaviour, upon irradiation at 241, 279 and 340 nm resulted in broad intense emission band at $\lambda_{max}$ =440 nm and a quantum yield of 50%. [60] Strong deep blue emission centred at 440 nm was observed upon photoexcitation of dithiadiazolyl pyrene in solution. Incorporation of dithiadiazolyl pyrene in different concentration as emissive component was incorporated into a PMMA matrix film to fabricate an OLED device. An acetonitrile solution of dithiadiazolyl phenanthrene radical revealed in the emission spectra a broad emission profile with a $\lambda_{max}$ = 410 nm and quantum yield of 11%. Radical polymer composites were formed to make a smooth film. Radical polymer concentration of 1:300 (w/w) results in emission spectra consisting of emission band at 380 nm and a shoulder at 420 nm. Increase in concentration of the radical in the polymer matrix causes an increase in weak emission band at 420 nm, which can be attributed to the excimer formation. DTDA radicals are well known to form a dimer in solution, especially at higher concentrations. [61–63] Thus a polymer composite should have lower radical concentration to avoid weaker emission bands at 420 nm. It can be concluded that the combination of PAHs and thiadiazolyl radical opens new possibilities for developing interesting photoluminescent materials.

## 1.6 Nitronyl Nitroxide Radical

Most often the free radicals are known to quench the fluorophore emission through electron or energy transfer process. [64–67] Nitronyl nitroxide radical belongs to a known class of stable radicals which are readily prepared from aldehydes mostly. This radical has been extensively used as stable spin labelling techniques. A great deal of studies has been done involving composite systems having metal

ions and nitronyl radical as ligative spin sources. [68–74] Mercury complexes bearing such nitronyl radical as ligands has been reported by Leute and Ullman. [75] Heavy metals such as Pt is chosen to attach with the stable radicals because they affect the luminescent properties significantly by accelerating ISC because of its high SOC [76]. This is quite challenging because the metal coordination usually quenches the luminescence of the radical ligand as it is known from literature that carboxylate ligands upon coordination with metal ions loses its luminescence properties.[77,78]

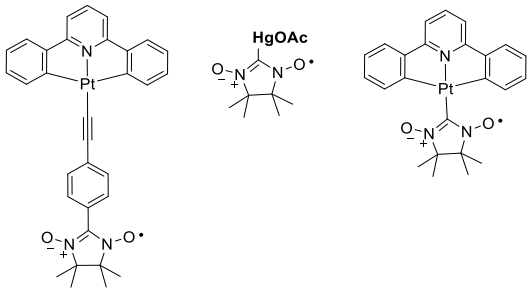


**Figure 13.** Structures of the complexes bearing nitronyl nitroxide radical ligand[79]

## 1.7 Luminescent Au(III) Complexes

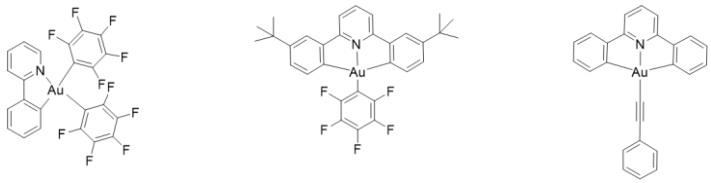

**Figure 14.** Structures of mono and biscyclometalated Au(III) complexes synthesized by our group [80,81]

Gold chemistry has been attracting researchers worldwide due to its stability, low toxicity and environmentally benign nature. Gold complexes are carbophilic Lewis acids which have the tendency to activate π-systems of alkenes, alkynes, allenes thus causing broad range of transformations to occur based on the strong relativistic effects.[82–88] Major drawback with organogold complexes is the presence of low lying d-d ligand field states in the case of gold(III) complexes which deactivates the excited states non-radiatively. Also, the electrophilic nature of the Au(III) centre might result in photodecomposition of excited states or result in other side reactions. Additionally the high redox potential of Au(III) causes reductive elimination. [89,90] On the other hand, higher SOC constant of gold could enhance ISC furthermore leading to the radiative decay of the triplet excited states. Luminescent properties of gold(III) complexes have been investigated based on monocyclometalated and biscyclometalated ligand scaffolds completed by an aryl or alkyne ligand around the coordination sphere. [91–94] Based on these basic fragments, a number of complex es with high emission quantum yields and reasonable device efficiency has been accomplished. However, one of their drawbacks in

comparison to the iridium(III) and platinum(II) complexes is their long excited triplet state lifetimes. We hypothesize that this can be mitigated through the introduction of stable radicals in the form of ancillary ligands to complete the coordination sphere around the gold(III) centre.

## 1.8 Luminsecent Pt(II) complexes

Platinum(II) complexes which are isoelectronic with Au(III) complexes have lower redox potential which makes Pt(II) complexes thermally more stable. Complexes bearing Pt(II) as the metal centre are most commonly known emitters and are frequently used in applications such as OLEDs, biosensors, biological imaging, photochromic materials. [95–105] Both Au(III) and Pt(II) with $d^8$ configuration stabilises in square planar geometry which give rise to intermolecular $\pi$-$\pi$, metal-$\pi$ and metal-metal stacking interaction that might lead to deactivation of the excited states and result in quenching of emission. On the other hand, such interactions might lead to the exciplex formation and provide ways for generating new luminescent materials. [106,107]

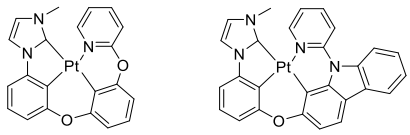


**Figure 15**. Structures of luminescent Pt(II) complexes. [108]

Moreover there are known Pt(II) pincer complexes which have excellent luminescent properties based on their robust ligand scaffold. [106,109] Phosphorescent behaviour displayed by platinum complexes at room temperature is due to its high spin orbit coupling constant, which allows singlet-triplet intersystem crossing and results in emission from the triplet excited state. Strong sigma donating nature of the cyclometalating ligand raises the low-lying d-d orbitals of the platinum thereby reducing the undesired non-radiative transitions and enhances phosphorescence quantum efficiency. [81,110–119]

## 1.9 Goal of the Thesis

Gold(III) complexes with ligands that have radicals are unprecedented and there are only a small number of Pt(II) complexes with ligands having radicals. The goal of this work is to synthesize Au(III) and Pt(II) complexes attached with nitronyl nitroxide radical ligand and PyBTM ligand, respectively and to investigate their structural and photophysical properties. The specific goal of the present study is to investigate the impact of radical ligand over the emissive properties of the Au(III) and Pt(II) complexes. Previously in our group luminescent monocyclometalated Au(III) complexes bearing aryl, alkyne, cyanide or aryl alkyne ligands were synthesized and their photophysical properties were studied. The Au(III) and Pt(II) complexes with the radical ligands is expected to result

in unique emission properties due to the interaction of radical with the charge-transfer state of the Au(III) and Pt(II) complexes. The new knowledge gained through the photophysical elucidation of the interplay between the radical spin and metal complexes is expected to lead to an efficient strategy for altering the excited-state properties of luminescent materials which could lead to potential applications for efficient light emitting devices. In addition, we also expect to unravel how the presence of a persistent radical impacts the excited state lifetime of the metal complex through interaction with the excited triplet state.

# 2 Results and Discussion

## 2.1Target Complexes

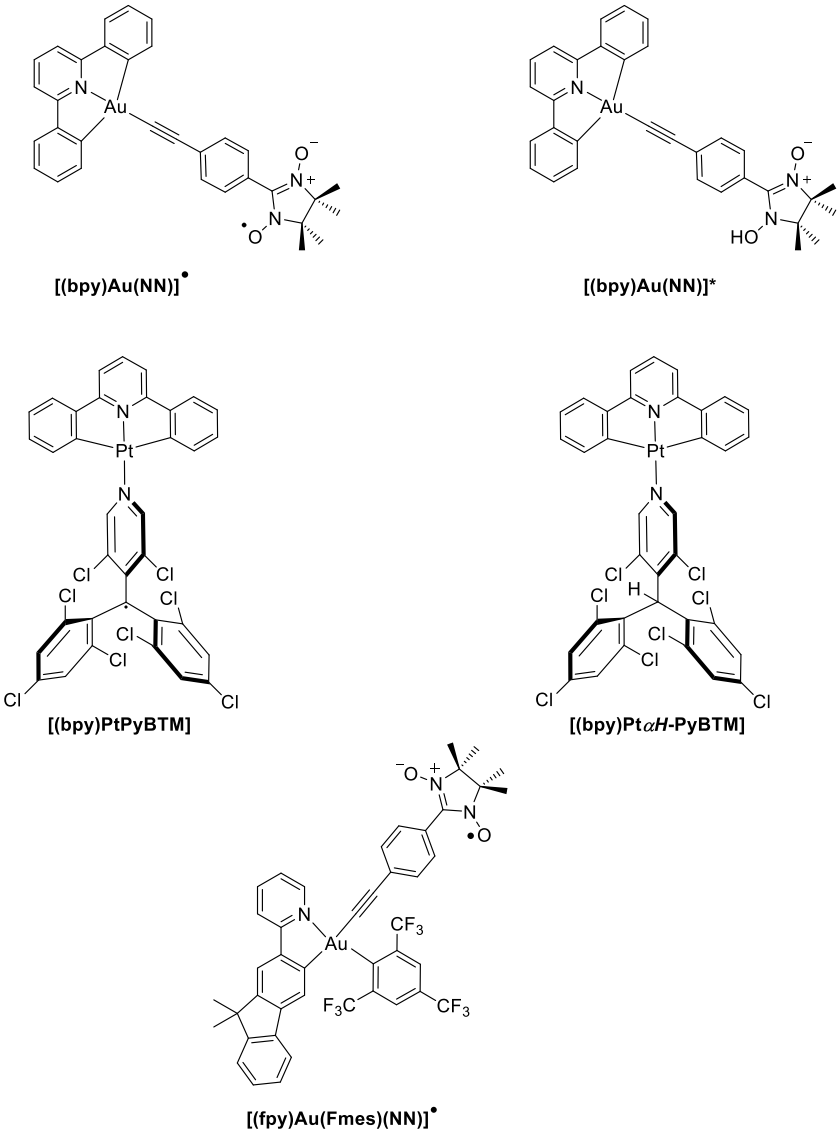


**Figure 16.** Structures of the synthesized complexes.

The final complexes shown in figure 16 were successfully synthesized and characterized. In all complexes, the metal centre is bound by a mono- or bis-cyclometalated ligand and an organic ancillary ligand **(α*H*-PyBTM and NN**) as well as their corresponding stable radical species (PyBTM and **NN˙**). The photophysical properties changes observed between a non-radical/radical pair will be discussed in the following sections.

## 2.2 Synthesis and Characterization of the Organic Ligands

### 2.2.1 2-(4-ethynylphenyl)-4,4,5,5-tetramethylimidazolidine-1,3-diol (NN Ligand)

Nitronyl nitroxide radical ligand was prepared by Sonoghashira cross coupling between commercially available 4-bromobenzaldehyde and trimethylsilylacetylene in the presence of palladium and copper catalyst. Treatment of silylated benzaldehyde with $K_2CO_3$ results in 4-ethynylbenzaldehyde which on condensation with **3** yielded **NN** which was characterized by $^1$H-NMR. This was further oxidised in presence of $NaIO_4$ to yield the desired radical compound NN˙ which was characterized by HR-ESI-MS. The general mechanism of the condensation is shown in scheme **1**. [120–122]

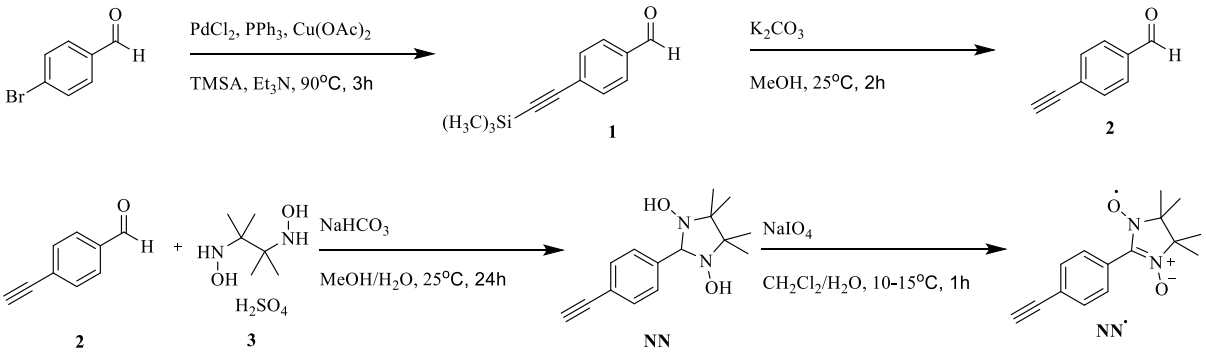


**Scheme 1**. NN˙ radical synthesis.

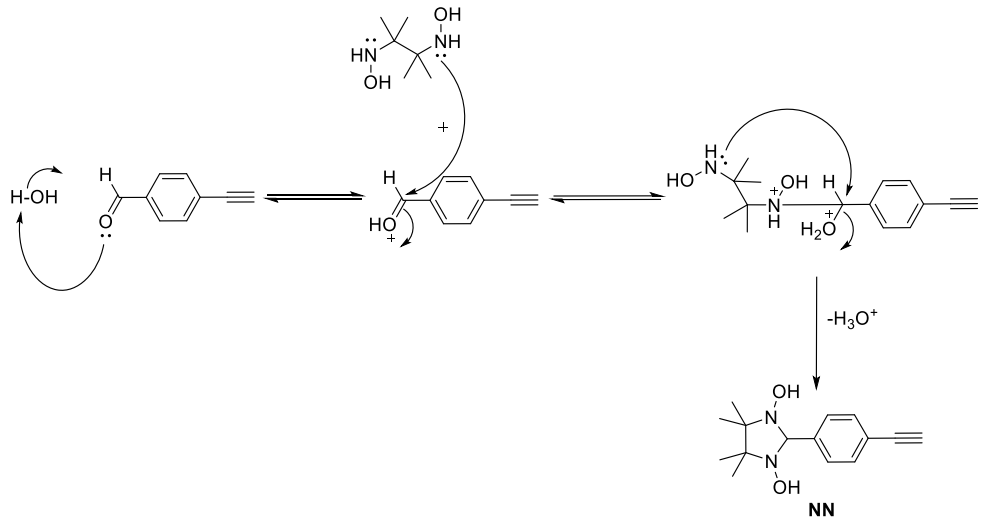


**Scheme 2**. Mechanism for Mannich-type reaction for NN formation.

This condensation is an example of Mannich-type reaction which requires an aldehyde and an amine and, in such reactions, the lone pair at the nitrogen attacks the carbonyl carbon. Further dehydration of the intermediate results in the formation of the condensed product **NN,** which was further oxidised

to **NN˙** using $NaIO_4$ as oxidising agent. This oxidation involves the formation of a cyclic periodate intermediate as shown in **scheme 3.** The radical was further purified by column chromatography on $Al_2O_3$ using $CH_2Cl_2$/Hexane as eluent (1:1). Mass spectrometry studies confirmed the mass peak at m/z 257.12830 for the $[M+H]^+$ species.

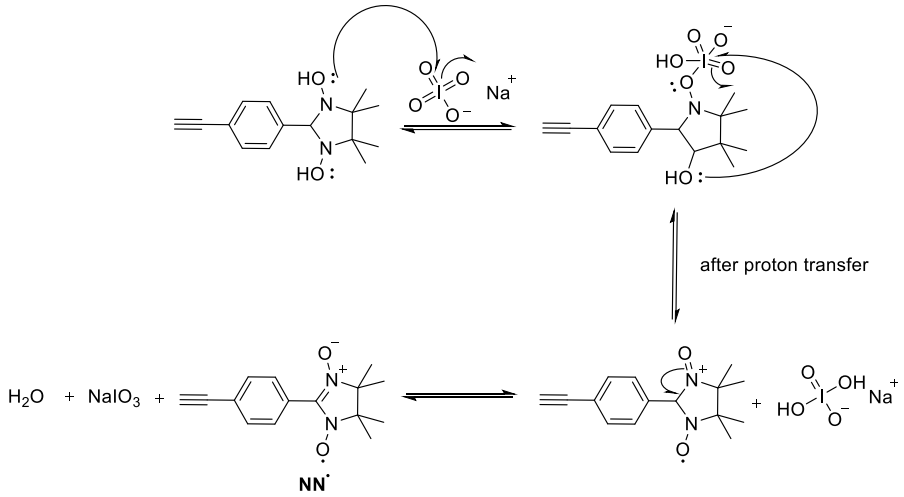


**Scheme 3.** Mechanism for NN˙ formation.

### 2.2.2 3,5-dichloro-4-pyridyl)bis(2,4,6-trichlorophenyl)methane (α*H*-PyBTM)

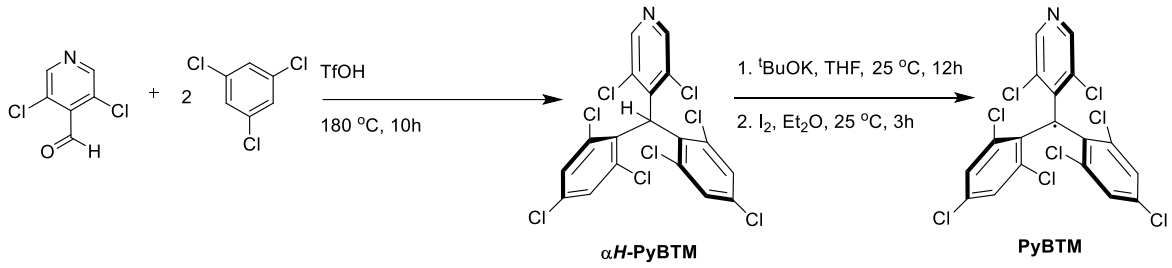


**Scheme 4**. Synthesis of PyBTM radical

3,5-dichloropyridine carboxaldehyde was refluxed with 1,3,5-trichlorobenzene in the presence of trifluoroacetic acid. The resulting reaction mixture was neutralized with $NaHCO_3$ and the aqueous layer was extracted with $CH_2Cl_2$ to give α*H*-PyBTM in a good yield. This superacid catalysed condensation of pyridine carboxaldehyde with arenes substituted with electron withdrawing groups proceeds via formation of carboxonium ions in the presence of Bronsted acid. [123–126]

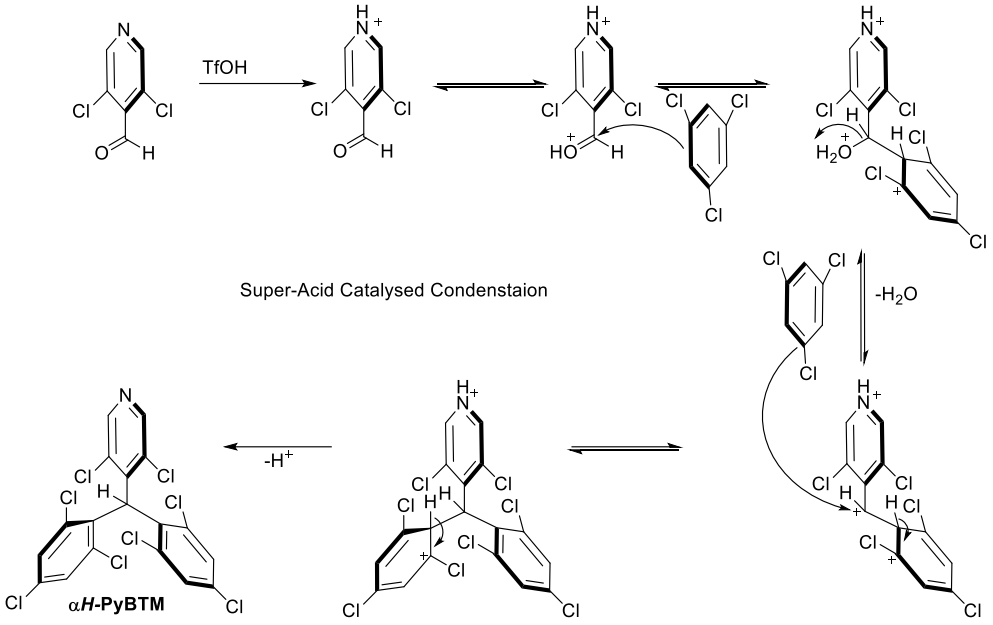


**Scheme 5.** Mechanism for *aH*-PyBTM formation.

This condensation depends remarkably over the acidity of the reaction system. Strong acid cause protonation of the carbonyl oxygen to produce a highly electrophilic benzaldehyde carbon. The superacid $CF_3SO_3H$ has proven to be an excellent catalyst for this condensation. [127,128] To decrease the neighbouring group participation, further protonation is required which will increase the electrophilic reactivity of the carbonyl carbon. The carboxonium ion generated is stabilised by the phenyl participation, which can be reduced by further protonation to enhance the electrophilic reactivity of the carbonyl carbon.[127] The dicationic electrophile have stable cationic centre adjacent to the cationic electrophilic site and can react with saturated as well as unsaturated hydrocarbons. Further oxidation of α*H*-PyBTM using $^t$BuOK and iodine generates the PyBTM radical. The addition of aqueous $Na_2S_2O_3$ solution washes away the excess iodine. The general mechanism of the radical formation occurs via deprotonation followed by oxidation as shown in scheme 6. The synthesized α*H*-PyBTM was characterized by $^1$H NMR and the radical compound PyBTM was characterized by HR-ESI-MS, showing the distinctive singlet of the tertiary proton at 6.71 ppm and the characteristic m/z 520.80215 for the $[M+H]^+$ species for PyBTM .[123]

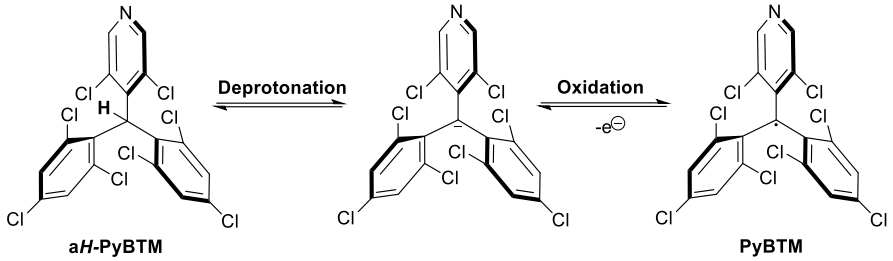


**Scheme 6.** Mechanism for PyBTM formation.

## 2.3 Synthesis and Characterization of the Final Complexes

The synthetic route for the target complexes is based on previous synthetic strategies discovered by our group and the literature [91–94,110]. An overview of the reaction cascade is shown in Scheme 7. Key step in the procedure of the final compounds are the ligand substitution reactions with the radical ligands proved to be extremely challenging due to the limited characterization methods for paramagnetic compounds.

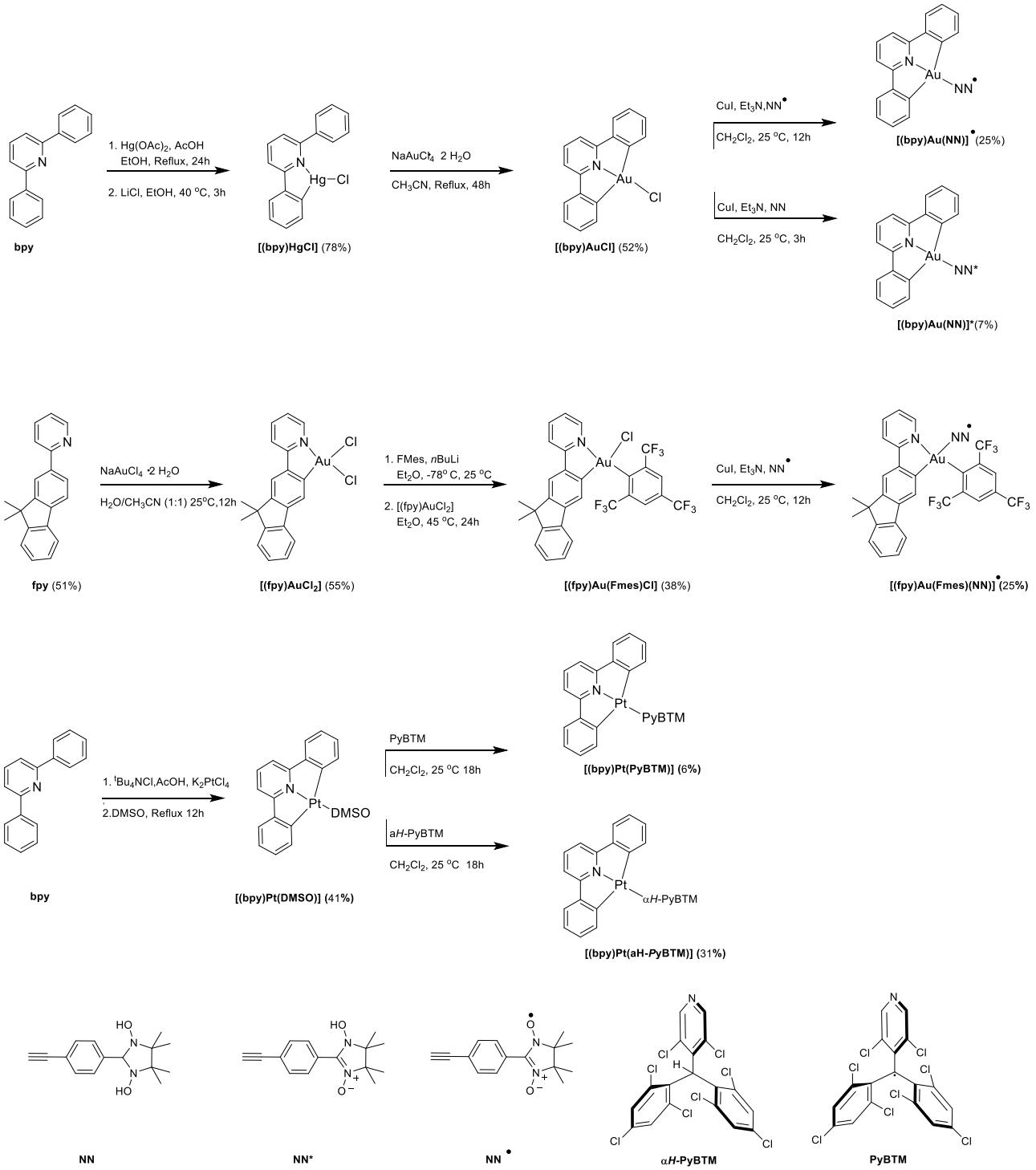


**Scheme 7**. Synthesis of final complexes. [91,106,109,129–135]

### 2.3.1 Biscyclometalated Au(III) Complex

The transition metal-mediated activation of a C-R bond to form a metallacycle comprising a new metal-carbon σ bond is termed as cyclometalation. Initially the donor group coordinates to the metal centre and subsequently intramolecular activation of C-R bond closes the metallacycle. Au(III) ions were transmetalated by reaction of biphenylpyridine with Hg(II) acetate followed by addition of ethanolic solution of LiCl to yield a colourless solid in a good yield, which on refluxing with $NaAuCl_4.2H_2O$ in $CH_3CN$ precipitated a pale yellow solid in a moderate yield and was characterized by $^1$H-NMR. Further alkynylation of **[(bpy)AuCl]** and **[(fpy)AuClFmes]** with **NN** and **NN˙** was carried out via copper acetylide transmetallation. The alkyne in **NN** and **NN˙** was first converted to copper acetylide in the presence of CuI and triethylamine (3 equivalents) in dry $CH_2Cl_2$ as solvent. The reaction proceeded well in good yield for the attachment of the **NN˙** to the Au(III) complex. The characterisation of the final Au(III) complexes bearing the radical ligand was done by HR-ESI-MS, elemental analysis and EPR. In contrast to this the reaction did not work at all with same amount of CuI with **NN** and generated iodine substituted Au(III) complex. Moreover, catalytic amount of CuI for the alkynylation of Au(III) complex with NN resulted in an emissive compound **[(bpy)Au(NN)]*** albeit in poor yield instead of the target structure **A** due to the easy oxidation of the dihydroxy adduct to the monohydroxy adduct.[136] Another possible reason for such product is that the slightly acidic protons of N-hydroxy group and tertiary carbon is easily abstracted by the base thereby resulting in an monohydroxy adduct. The obtained product **[(bpy)Au(NN)]*** was confirmed with $^1$H-NMR which clearly shows the absence of one of the hydroxy proton and one proton on tertiary carbon. The HR-ESI-MS shows characteristic mass peak *m/z* at 684.19113. It was found out to be emissive and while the complex bearing the radical was non-emissive which is probably due to the quenching effect of the radical. The complex [(bpy)Au(NN)]˙ was also confirmed by HR-ESI-MS showing a distinctive mass peak *m/z* at 682.17553.

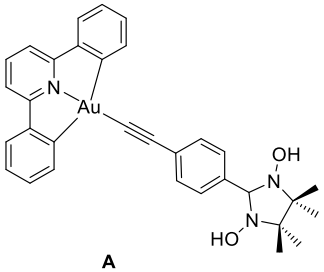


A

**Figure 17.** Structure of targeted [(bpy)Au(NN)] complex.

### 2.3.2 Monocyclometalated Au(III) Complex

Suzuki coupling of **4** with bromopyridine in DME/EtOH gives **fpy** which upon further reaction with $NaAuCl_4 \cdot 2H_2O$ in $CH_3CN$ gave **[fpyAuCl$_3$]**. Thereafter cyclometalation of **[fpyAuCl$_3$]** gave $fpyAuCl_2$. This was further treated with lithiated FMes to give the monoarylated gold(III) complex **[(fpy)AuCl]Fmes** in a moderate yield.[91,93] Similarly **[(fpy)Au(Fmes)NN$^{\bullet}$]** was synthesized successfully with CuI and triethylamine (3 equivalents) in dry $CH_2Cl_2$ via copper acetylide formation. The crude product was purified by column chromatography on $Al_2O_3$ using $CH_2Cl_2$/Hexane as eluent. The obtained product was confirmed by HR-ESI-MS and shows characteristic mass peak at *m/z* 1005.22208. **[(fpy)AuFmes(NN)]** did not form under the same reaction conditions. In conclusion gold(III) complex bearing **NN$^{\bullet}$** radical could be achieved due to better stability for alkynylation than the non-radical **NN** which is quite unstable under basic reaction conditions and leads to other undesirable products. Moreover, the **[(fpy)Au(Fmes)Cl]** complex is found to be less reactive due to the deactivating Fmes group which leads to slower reaction, while the ligand undergoes a faster side reaction.

### 2.3.3 Biscyclometalated Pt(II) Complex

This cyclometallation proceeds when 2,6-diphenylpyridine is refluxed with $K_2PtCl_4$ in presence of $^{t}Bu_4NCl$ and AcOH. The monocyclometalated complex initially formed undergoes loss of HCl to result in the biscyclometalated complex **[(bpy)PtDMSO]** in the presence of a polar solvent such as DMSO, which was characterized by $^{1}$H-NMR. [106]After that the **[(bpy)PtDMSO]** complex was reacted via simple ligand exchange reaction by substituting DMSO with **α*H*-PyBTM** in dry $CH_2Cl_2$. The compound was purified to deliver **[(bpy)Pt(α*H*-PyBTM)]** which was confirmed by HR-ESI-MS ,$^{1}$H-NMR and $^{13}$C-NMR. The $^{1}$H-NMR spectra of **[(bpy)Pt(α*H*-PyBTM)]** displays a singlet slightly deshielded from 6.71 ppm to 6.77 ppm for the proton attached to the tertiary carbon of the ligand, which is probably due to the coordination of the ligand to the metal complex. The HR-ESI-MS spectra of **[(bpy)Pt(α*H*-PyBTM)]** clearly shows distinctive mass peak at *m/z* 941.86859. Similarly, **[(bpy)Pt(PyBTM)**] was synthesized via ligand exchange reaction of **[(bpy)Pt(DMSO)]** with PyBTM and further purified by column chromatography on $Al_2O_3$ and characterized by HR-ESI-MS with a characteristic mass peak at *m/z* 939.85820 .

## 2.4 Electron Paramagnetic Resonance (EPR) Studies

The EPR Spectra of final complexes and radical ligands were recorded in $CH_2Cl_2$ at room temperature. The samples were diluted until line narrowing ceased and all the simulations were performed in easyspin. The spectra did not reveal any significant amount of coupling between free radical and the gold atom and resembles more like the spectra of the free ligand as shown in figure 18.

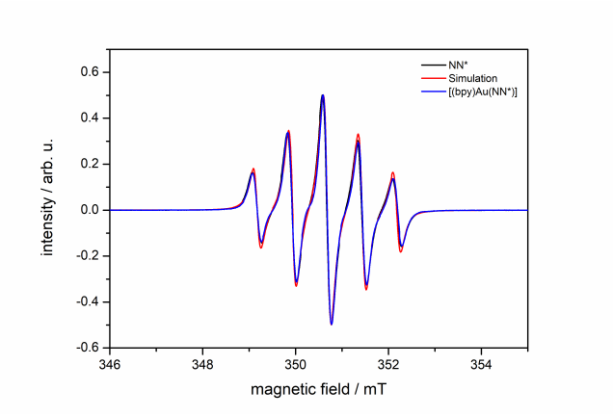


**Figure 18**. EPR spectra of measured and simulated **[(bpy)Au(NN)]˙ and NN˙.**

Simulation for the complex **[(bpy)Au(NN)]˙** was not explicitly done but plotted against the simulation of **NN˙** to show that they are essentially identical. It is possible to simulate both the spectra together if we treat both the nitrogen nuclei's equally as they are equivalent (same hyperfine splitting) we get equally good simulations. The EPR spectra of the complex **[(bpy)Au(NN)]˙** does not show any visible evidence of the unpaired electron of the nitrogen ligand coupling to that of gold atom because the spectra looks similar to that of spectra of the free ligand **NN˙**. The g factor and coupling constant values are provided in table 1. However, this does not exclude the presence of Au atom. If the hyperfine splitting caused by Au is extremely small, the splitting could be difficult to observe in the linewidth of the spectrum. Specifically, if Au is less than a quarter of the linewidth it would not be observed. Additionally, it should also be taken into consideration that the EPR spectra alone cannot prove the presence of Au atom in the system.

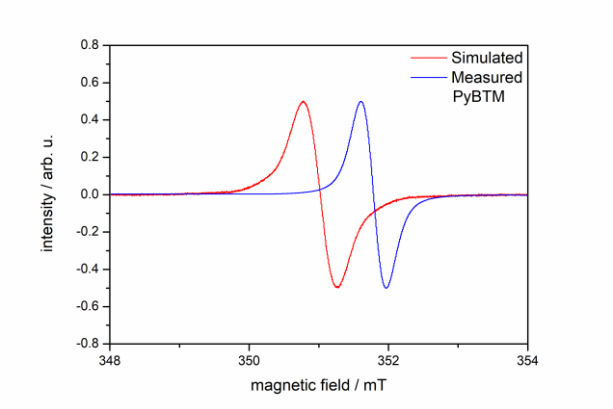


**Figure 19**. EPR spectra of measured and simulated PyBTM radical.

The EPR spectra of the PyBTM also reveals the presence of the paramagnetic species which was obvious as shown in figure 19. The EPR spectra of the platinum complex shows the presence of the radical within the complex and comprised of two distinct signals one of which resembles the free radical PyBTM whereas the slightly narrower one shows coupling to the Pt nucleus and reveals the coupling $|a_{Pt}| = 2.8$. However with these results it is not clear if the electron is delocalised across the ligand and the Pt centre or it is shifted to the metal centre.[137] Further experiments and DFT calculations are required in order to arrive at further conclusion.

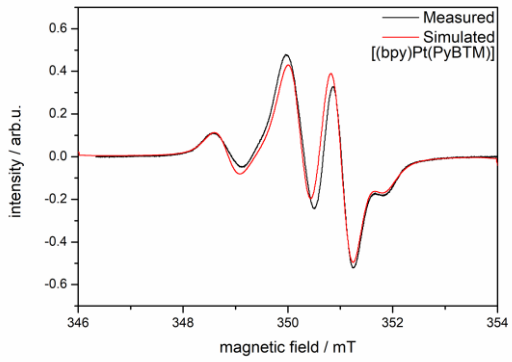


**Figure 20**. Measured and simulated EPR spectra of [(bpy)Pt(PyBTM)].

| **Sample** | **Isotropic g-factor** | **a(N)$_1$** mT [s.p][1] | **a(N)$_2$** mT (s.p)[1] | **a(Au)** mT | **a(Pt)** mT |
|---|---|---|---|---|---|
| NN$^{\bullet}$ | 2.007 | 0.74 [20%] | 0.77 [21%] | - | - |
| [(bpy)Au(NN)]$^{\bullet}$ | 2.007 | 0.74 [20%] | 0.77 [21%] | 0 (<0.06) | - |
| PyBTM | 2.004 | - | - | - | - |
| [(bpy)Pt(PyBTM) | 2.006 | - | - | - | 2.80 [25%] |

**Table 1.** g and $|a|$ values are summarised from EPR studies.

## 2.5 Photophysical Studies

### 2.5.1 UV-Vis and Emission Spectra of Au(III) Complexes

The UV-Vis spectra of the ligands and the final complexes were measured in $CH_2Cl_2$ solution. The significant differences of the absorption profiles show that the electronic properties are mainly influenced by the presence of the radical ligand. The **NN˙** shows characteristic absorption bands at 320, 337 and 383 nm which is in agreement with the reported literature. The monocyclometalated **[(fpy)Au(Fmes)(NN)]˙** shows maximum extinction coefficient in the visible region than **[NN]˙** and **[(fpy)Au(Fmes)(Cl)]** as shown in figure 21. Similar behaviour is seen with the biscyclometalated Au(III) complex **[(bpy)AuNN)]˙** shown in figure 22.

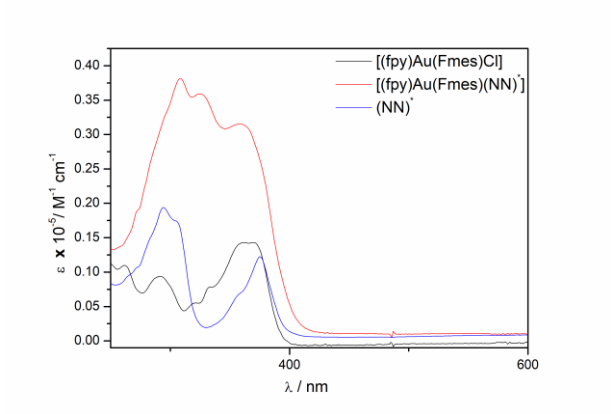


**Figure 21.** UV-Vis spectra of complexes **[(fpy)Au(Fmes)Cl]** and **[(fpy)Au(Fmes)(NN)]˙** with ligand **NN˙.**

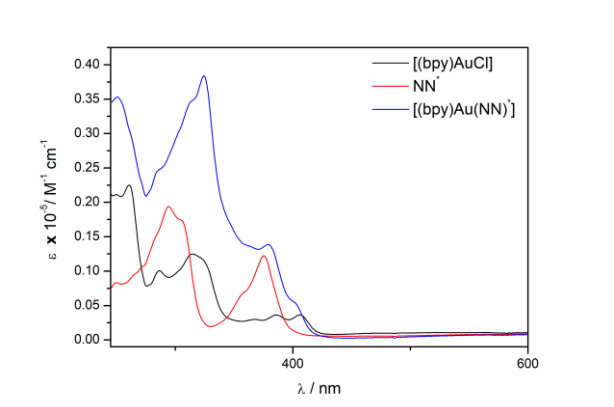


**Figure 22.** UV-Vis spectra of complexes **[(bpy)AuCl]**, **[(bpy)AuNN)]˙** and ligand **NN˙**.

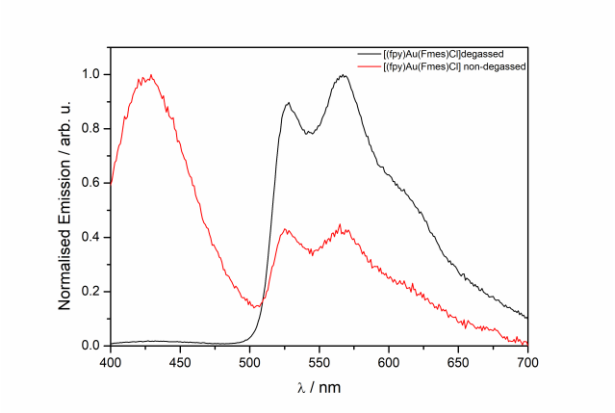


**Figure 23.** Emission spectra of degassed and non-degassed solution of **[(fpy)Au(Fmes)Cl]**.

The emission study was done in degassed $CH_2Cl_2$ solution for all the final complexes and the ligands. Figure 23 shows the emission profile of the monocyclometalated complex **[(fpy)Au(Fmes)Cl]** and it can be concluded from the spectra that the degassed solution of the complex shows phosphorescence which seems to get quenched in the case of non-degassed solution. The possible explanation for such observation is the interaction of triplet oxygen with the triplet excited states which results in appreciable amount of phosphorescence quenching. The noise in the red spectra clearly shows very weak phosphorescence which gets enhanced on degassing the solution. Similarly the emission spectra shown in figure 24 reveals quenching of phosphorescence due to the presence of the paramagnetic species in **[(fpy)Au(Fmes)(NN)]˙**.

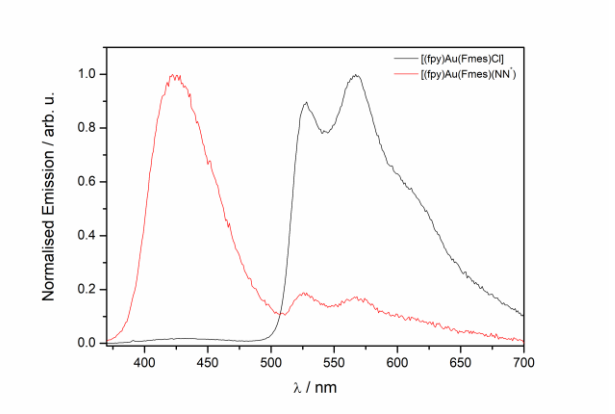


**Figure 24.** Emission Spectra of **[(fpy)Au(Fmes)Cl]** and **[(fpy)Au(Fmes)(NN)]˙**.

The emission profile for **[(fpy)Au(Fmes)(NN)]˙** shows weak emission at $\lambda_{em}$ =424 nm and shows diminishing phosphorescence due to quenching effect of radical. The biscyclometalated Au(III) complex [(bpy)AuCl] is emissive in solution as known from the literature, whereas complex **[(bpy)Au(NN)]˙** was also found out to be non-emissive due to similar reasons. [131,138]

## 2.5.2 UV-Vis and Emission Spectra of Pt(II) complexes

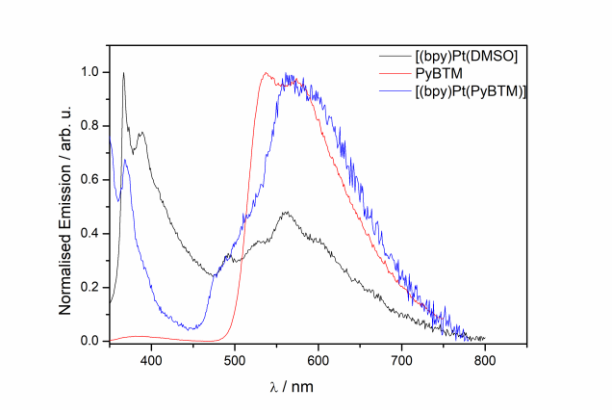


**Figure 25.** Emission spectra of **[(bpy)Pt(DMSO)]**, **PyBTM** and **[(bpy)Pt(PyBTM)].**

The ligand **PyBTM** itself due to larger delocalised system has lower $\pi - \pi$ transitions and thus possess low energy transitions (bathochromic shift) at room temperature. The spectra shows a weak emission for **[(bpy)Pt(PyBTM)]** at $\lambda_{em}$ = 580 nm whereas the **[(bpy)Pt(DMSO)]** shows extremely weak emissions and lifetime for such weak emissions could not be measured as shown in figure 25. The emission profile for the ligand and the final complex looks similar. It is therefore difficult to say if the ligand alone is causing such emission or if there is also participation of the metal. It was expected that sufficiently high SOC of Pt(II) might result in fast ISC and result in radiative decay of the triplet states, however this was not observed in room temperature measurements. Temperature dependent measurements and DFT calculations are further required in order to unravel the emission behaviour of the complexes.

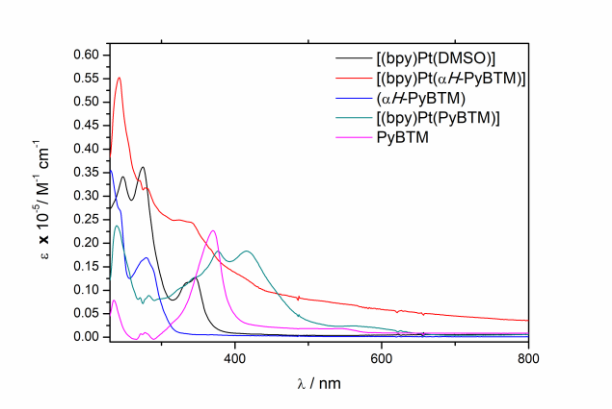


**Figure 26.** UV-Vis spectra of the ligand and Pt complexes.

The UV-Vis spectra of the synthesized Pt(II) based complexes and the ligands is shown in figure 26, where the transitions of the ligand **α*H*-PyBTM** is shown in blue, while the transitions for the **PyBTM** shown in visible region also resembles with the reported literature.[8] The **[(bpy)Pt(DMSO)]** complex

has transitions around 375 nm and the transitions for the **[(bpy)Pt(PyBTM)]** is significantly red shifted in comparison. This can be explained based on an assumption that because of extended $\pi$ conjugation due to **PyBTM** radical, there is a decrease in HOMO-LUMO gap causing this significant red shift.

| **Complex** | **Absorption** $\lambda_{max}$/nm($\varepsilon$/$M^{-1}cm^{-1}$) | **Medium (T/K)** | **Emission** $\lambda_{max}$/ nm | **Lifetime in Solution** $\mu$s |
|---|---|---|---|---|
| **[(fpy)Au(Fmes)Cl]** | 292 (9397)<br>366 (14217) | $CH_2Cl_2$ [298] | 527<br>567 | 30.2<br>129.5 |
| **[(bpy)Pt(PyBTM)]** | 230 (12188)<br>270 (8315)<br>351 ( 13032) | $CH_2Cl_2$ [298] | - | - |
| **[(bpy)Au(NN)]˙** | 325 (38329)<br>381 (13665) | $CH_2Cl_2$ [298] | - | - |
| **[(fpy)Au(Fmes)(NN)]˙** | 356 (31456) | $CH_2Cl_2$ [298] | 424 | - |
| **[(bpy)Pt(αH-PyBTM)]** | | $CH_2Cl_2$ [298] | | |
| **PyBTM** | 360 (19634) | $CH_2Cl_2$ [298] | 587 | $6.3*10^{-3}$ |
| **[(bpy)Pt(DMSO)]** | 342 (12566) | | 367<br>389<br>562 | |

**Table. 2** Photophysical properties of all the final complexes**.**

## 2.6 Conclusion and Outlook

Organic radicals are a tremendously emerging field of research as they are being considered as next generation fluorophore whereas earlier they were known to quench fluorescence. In a view to expand the emerging field of luminescent organic radicals, structural modifications like introducing an electronegative atom, electron withdrawing groups, transition metal ions, carbazole moiety, have already been proven as an effective way to enhance the quantum yield and photostability. In this work we show the synthesis and characterization of monocyclometalated gold(III), biscyclometalated gold(III) and biscyclometalated Pt(II) complexes with persistent radicals. It is important to mention that the these are the first examples of gold(III) complexes bearing radical ligands. The neutral complexes have also been synthesized and characterized in the case of biscyclometalated gold(III) and biscyclometalated Pt(II) complex. All the final complexes were found to be stable at ambient conditions. EPR measurements confirmed the presence of the radical in the final complexes and the respective interaction with the metal centre. To further study the exact position of the radical in the final Pt complex some pulsed (ESEEM / ELDOR) experiments will be carried out in the future. Photophysical measurements revealed the complexes to be non-emissive in solution at room temperature. Further luminescence measurements will be carried out to ascertain their excited state behaviour at low temperature and in thin films. The redox and magnetic behaviour will be ascertained through electrochemical and magnetic susceptibility measurements. The new knowledge gained through the elucidation of their electronic properties is expected to throw light on the interplay between the radical spin and the central metal. This is further expected to lead to an efficient strategy for altering the excited-state properties of luminescent materials which could then lead to applications of these new molecular systems in efficient light emitting devices.

# 3 Experimental Part

## 3.1 Materials and Equipment

Unless otherwise stated, all manipulations were carried out without special precautions for excluding air and moisture. $^{1}$H-, $^{13}$C- and $^{19}$F-NMR were recorded on either *Bruker* AV-500 and AV-400 spectro-meters at constant temperature of 298 K. Chemical shifts (δ) are reported in parts per million (ppm) referenced to tetramethylsilane (δ 0.00 ppm) using the residual protio solvent peaks as internal standards ($^{1}$H-NMR experiments) or the characteristic resonances of the solvent nuclei ($^{13}$C-NMR expmeriments). Coupling constants (*J*) are quoted in hertz [Hz], and the following abbreviations are used to describe the signal multiplicities: *s* (singlet); *br s* (broad singlet); *d* (doublet); *t* (triplet); *q* (quatruplet); *sept.* (septet); *m* (multiplet); *dd* (doublet of doublet); *dt* (doublet of triplet). Proton and carbon assignments have been made using routine one and two-dimensional NMR spectroscopies where appropriate. Chromatographic purification of products was performed on a short column (length 15.0 cm: diameter 1.5 cm) using forced flow of eluent. High-resolution mass spectrometry was performed on a Q Exactive Plus (Thermo Scientific, San, Jose, USA) which is an Orbitrap platform mass spectrometer and utilises heated electron spray ionization probe, operated in positive as well as negative ion mode. Elemental microanalysis was carried out with *Leco CHNS-932* analyser. TLC analysis was performed on precoated *Merck* Silica Gel 60$F_{254}$ slides, Macherey Nagel ALOX N/$UV_{254}$ and visualized by luminescence quenching either at 254 nm or 365 nm. UV-Vis measurements were carried out on a *Perkin-Elmer Lambda 19* UV-Vis spectrophotometer. Emission spectra were acquired on an *Edinburgh FLS980* spectrophotometer using 450W Xenon lamp excitation by exciting at the longest wavelength absorption maxima. All samples for emission spectra were degassed by 15 min $N_2$ flow. All microwave reactions were conducted in an *Anton Paar Monowave 300 Synthesis* reactor. CW-X-Band EPR spectra were measured on a commercial Bruker E500 spectrometer equipped with a Bruker ER4122 SHQ resonator. Samples were loaded into conventional X-Band EPR tubes with an inner diameter of 2.8 mm. Spectra were measured at room temperature using 4.74 mW, 9.85 GHz microwaves and 0.5 G modulation amplitude, unless indicated otherwise Commercially available reagents were purchased from *Aldrich*, *Chemie-Brunschwig* and *Fluorochem* and were used as such without further purification.

## 3.2 Synthetic Procedures

1) 4-Trimethylsilylbenzaldehyde (**1**)[120–122]

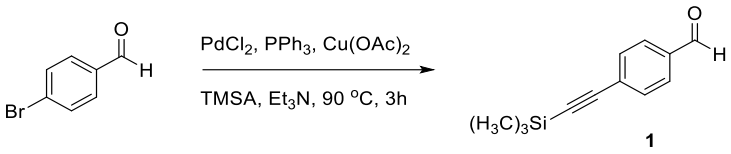


TMSA was added (8.1 g, 38.0 mmol) to a solution of 4-bromobenzaldehyde (10.0 g, 54.3 mmol), $PPh_3$ (0.71 g, 1.3 mmol), $PdCl_2$ (45 mg, 0.25 mmol), and $Cu(OAc)_2$ (0.1 g, 0.25 mmol) in 60 mL of anhydrous triethylamine at room temperature. The reaction mixture was refluxed for 3h. After cooling, the reaction mixture was extracted with $CH_2Cl_2$ (3 x 30 mL), the organic layer was separated, dried over $Na_2SO_4$ and the solvent was evaporated. The crude material was purified on a $SiO_2$ column using EtOAc/hexane (1:6) as eluent to give silylated aldehyde (7.0 g, 34.6 mmol, 63%). $^1$H-NMR (400 [MHz], $CDCl_3$, 25 °C): δ [ppm] = 10.00 (*s*, 1 H, -CHO); 7.82 (*m*, 2 H, -*arom.*); 7.60 (*m*, 2H, -*arom*); 0.27 (*s*, 9 H, -$SiCH_3$). The NMR data is consistent with the reported literature.

2) 4-Ethynylbenzaldehyde (**2**) [120–122]

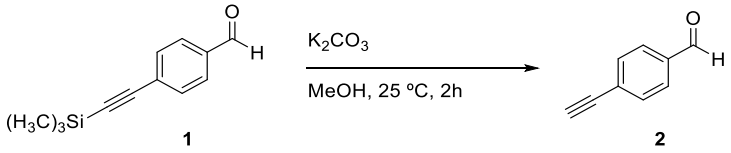


To a solution of 4-trimethylsilyl benzaldehyde (7.0 g, 34.60 mmol) in MeOH (30 mL), $K_2CO_3$ (0.48 g, 3.46 mmol) was added to it. The reaction mixture was stirred at 25 °C for 2h. The solvent was evaporated, the crude was dissolved in $CH_2Cl_2$(50 mL) and washed with aq. $NaHCO_3$. The combined organic layers were dried over $Na_2SO_4$ and concentrated to yield 4-ethynylbenzaldehyde (4.2 g, 35.5 mmol, 94%) as an orange colour solid. $^1$H-NMR (400 [MHz], $CDCl_3$, 25°C): δ [ppm] = 10.02 (*s*, 1 H, -CHO); 7.85 (*m*, 2 H, -*arom.*); 7.64 (*m*, 2 H, -*arom.*), 3.29 (*s*, 1 H, -CCH). The NMR data is consistent with the reported literature.

3) 2,3-Bis(hydroxyamino)-2,3-dimethylbutane sulphate (**3**).[74,121]

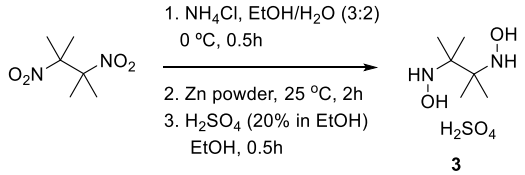

A cooled solution of 2,3-dimethyl dinitrobutane (5.1 g, 28.4 mmol) and $NH_4Cl$ (3.0 g, 56.8 mmol) in EtOH/$H_2O$ (3:2) was stirred for 30 minutes at (0 – 5 °C). Zinc (12.4 g, 189 mmol) was added slowly to the reaction mixture. After 30 min. the reaction mixture was allowed to warm up to room temperature and was stirred for 2h. The solid was filtered and washed with anhydrous ethanol. The filtrate was acidified with solution of $H_2SO_4$ in ethanol (10 mL, 20%) and additional 60 mL of anhydrous EtOH was added. The resulting mixture was stirred for 30 min. and the colourless precipitate was filtered to give **3** (3.4 g, 13.8 mmol, 49%) which was further used without purification.

4) 1,3-Dihydroxy-2-(4-ethynylphenyl)-4,4,5,5-tetramethylimidazolidine (**NN**)[122]

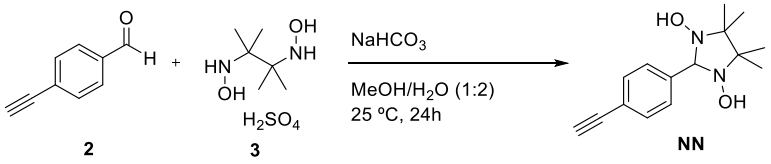


An aq. hot (50 °C) solution of **3** (3.6 g, 13.6 mmol) in $H_2O$ (20 mL) was added to a solution of aldehyde **2** (1.2 g, 9.1 mmol) in MeOH (13 mL) at 50 °C. After that the reaction mixture was stirred at 25 °C for 24 h and neutralized with $NaHCO_3$ (1.55 g, 18.5 mmol). The reaction mixture was extracted with $CH_2Cl_2$ (3 x 30 mL), the combined organic layers were dried over $Na_2SO_4$ and solvent was evaporated. The crude material was purified on a $SiO_2$ column using EtOAc/hexane (1:6) as eluent to give **NN** (0.48 g, 1.84 mmol, 20%) as the product. $^1$H-NMR (400 [MHz], DMSO, 25 °C): δ [ppm] = 7.79 (*s*, 2 H, -OH); 7.46 (*m*, 4 H, -*arom*.), 4.51 (*s*, 1 H, -CH-); 4.13 (*s*, 1 H, C≡CH), 1.05 (*d*, 12 H, -$CH_3$). The NMR data is consistent with the reported literature.

5) 2-(4-Ethynylphenyl)-4,4,5,5-tetramethyl-2-imidazoline-1-oxyl-3oxide (**NN**$^{\cdot}$)[122]

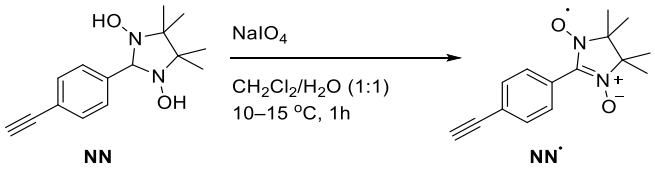


**NN** (0.32 g, 1.2 mmol) was dissolved in $CH_2Cl_2$ (20 mL) and cooled down to 0 °C. A solution of $NaIO_4$ (0.39 g, 1.8 mmol) in $H_2O$ (20 mL) was added to it and the reaction mixture was stirred at 10-15 °C for 1 h. The organic layer was separated and the aqueous layer was extracted with $CHCl_3$ (3 x 20 mL). The combined organic layers were dried over $Na_2SO_4$ and the solvent was evaporated. The crude product was purified with column chromatography on $Al_2O_3$ using $CH_2Cl_2$/Hexane (1:2) as eluent to deliver **NN**$^{\cdot}$ (135.0 mg, 0.5 mmol, 43%). (+)-HR-ESI-MS (MeOH): calcd for $C_{15}H_{17}N_2O_2^{\cdot}$ $[M+H]^+$:*m/z* 257.12902, found 257.12830.

6) **(3,5-dichloro-4-pyridyl)bis(2,4,6-trichlorophenyl)methane** (***αH*-PyBTM**).[4]

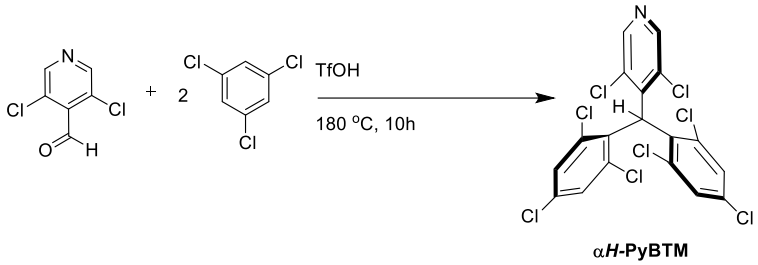


Under nitrogen atmosphere, 3,5-dichloro-4-pyridine carboxaldehyde (1.8 g, 10.0 mmol,) and 1,3,5-trichlorobenzene (18.1 g, 100 mmol) were heated to 180 °C. Trifluoromethanesulfonic acid (30.0 g, 20 mmol) was added dropwise, and the reaction mixture was stirred for 10 h at 180 °C. The reaction mixture was cooled to room temperature, dissolved in $CH_2Cl_2$ (50 mL) and added to ice water (50 mL). The mixture was neutralized to pH=7 using $NaHCO_3$, extracted with $CH_2Cl_2$ (3 × 100 mL), washed with aq. $NaHCO_3$ solution (2 x 50 mL), and dried over $Na_2SO_4$. The solvent was evaporated and the crude was purified by column chromatography on $SiO_2$ using $CH_2Cl_2$/Hexane (1:1) to afford pure ***αH*-PyBTM** (3.1 g, 6.0 mmol, 60%). ($^1$H-NMR (400 [MHz], $CDCl_3$, 25 °C): δ [ppm] = 8.48 (*s*, 1 H, -*arom.*), 8.36 (*s*, 1 H, -*arom.*), 7.39 (*d*, $J_{HH}$ = 2.4, 1 H, -*arom.*), 7.38 (*d*, $J_{HH}$ = 2.2, 1 H, -arom.), 7.27 (*d*, $J_{HH}$ = 2.2, 1 H, -*arom.*), 7.24 (*d*, $J_{HH}$ = 2.4, 1 H, -*arom.*), 6.69 (*s*, 1 H, -CCH). The NMR data is consistent with the reported literature.

7) **(3,5-dichloro-4-pyridyl)bis(2,4,6-trichlorophenyl)methyl radical** (**PyBTM**).[4]

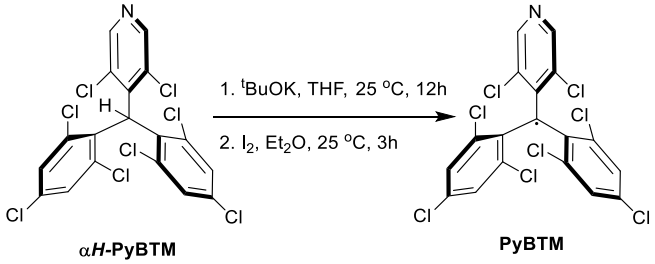


***αH*-PyBTM** (0.47 g, 0.9 mmol) was dissolved in dry THF (35 mL) under nitrogen atmosphere and $^t$BuOK in THF (1M, 1.4 mL, 1.4 mmol) was added. The reaction mixture was stirred overnight at 25 °C in the dark. To the reaction mixture, a solution of $I_2$ (1.3 g, 5.2 mmol) in dry $Et_2O$ (60 mL) was added dropwise at 25 °C and stirred for 3h. The remaining $I_2$ was washed by reducing with 10% $Na_2S_2O_3$ solution (3 x 30 mL). The water layer was extracted with $Et_2O$ and combined organic layers was dried over $Na_2SO_4$. The crude was purified by column chromatography on $Al_2O_3$ using $Et_2O$/hexane (1:4) and dried *in vacuo* to afford dark red PyBTM (0.34 g, 0.65 mmol. 72%). (+)-HR-ESI-MS (MeOH): calcd for $C_{18}H_6Cl_8N^{\cdot}$ $[M+H]^+$:*m/z* 520.80, found 520.80215.

8) 2-(9,9-dimethyl-9H-fluoren-2-yl)pyridine (**fpy**)[139]

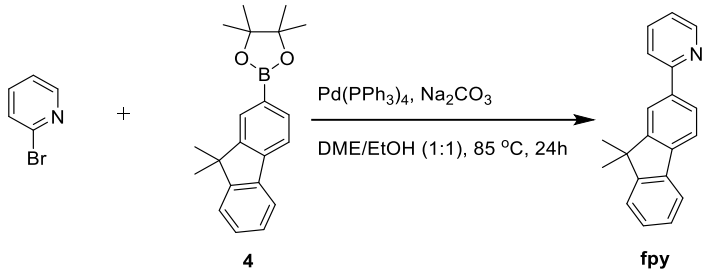


To a degassed mixture of DME (50 mL) and EtOH (50 mL), **4** (0.53 g, 1.6 mmol,), 2-bromopyrdine (0.2 g ,1.3 mmol) and 2M $Na_2CO_3$ (0.4 g, 3.9 mmol) was added and degassed again. Further $Pd(PPh_3)_4$ was added (0.6 g, 0.13 mmol) and the reaction mixture was heated to reflux for 24 h. The desired product was extracted with $CH_2Cl_2$ (3 x 30 mL). The combined organic layers were dried over $Na_2SO_4$. The solvent was evaporated, and the crude was purified by column chromatography on $SiO_2$ using $CH_2Cl_2$/hexane (1:2) to afford **fpy** (0.2 g, 0.8 mmol, 51%). $^1$H-NMR (400 [MHz], $CDCl_3$, 25 °C): δ [ppm] = 8.74 (*dd*, 1 H, $J_{HH}$ = 4.0,), 8.14 (*s*, 1 H, *arom.*), 7.95-7.98 (*dd*, 1 H, $J_{HH}$ = 8.0, 1.7, *arom.*), 7.81 –7.83 (*m*, 2 H, *arom.*), 7.76 – 7.79 (*m*, 4 H, *arom.*), 7.44 – 7.48 (*m*, 1 H, *arom.*), 7.34 – 7.37 (*m*, 2 H), 1.56 (*s*, 6 H, $CH_3$). The NMR data is consistent with the reported literature.

9) $[(fpy)AuCl_3]$.[140]

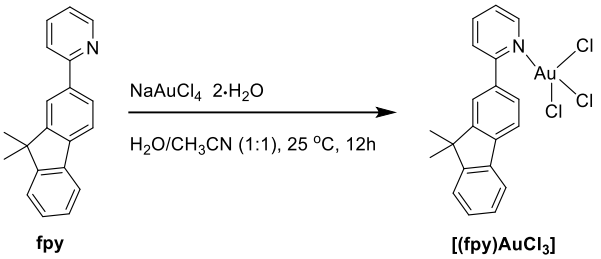


Equimolar amounts of **fpy** (0.2 g, 0.8 mmol) and $NaAuCl_4 \cdot 2H_2O$ (0.3 g, 0.8 mmol) were dissolved in a 1:1 mixture of $CH_3CN$ (6 mL) and $H_2O$ (6 mL). The reaction mixture was stirred overnight at room temperature. The precipitate was filtered, washed with $H_2O$ and dried *in vacuo* to get the desired product [**(fpy)AuCl$_3$]** (0.3 g, 0.5 mmol, 66%).

$^1$H-NMR (400 [MHz], $CDCl_3$, 25°C): δ [ppm] = 8.81 (*dd*, 1 H, $J_{HH}$ = 4, 0.5, py.), 8.20 (*m*, 1 H, $J_{HH}$ = 8, 1.3, *arom.*), 8.12 (*d*, 1 H, *arom.*), 7.90-7.94 (*td*, 2 H, $J_{HH}$ = 8, *arom.*), 7.80-7.82 (*dd*, 1 H, $J_{HH}$ = 4.0, 1.1, *arom.*), 7.68 – 7.71 (*m*, 2 H, *arom.*), 7.49 – 7.52 (*m*, 1 H, *arom.*), 7.40 – 7.42 (*m*, 2 H, *arom.*), 1.60 (*s*, 6 H, $CH_3$). The NMR data is consistent with the reported literature.

10) [(fpy)$AuCl_2$].[141]

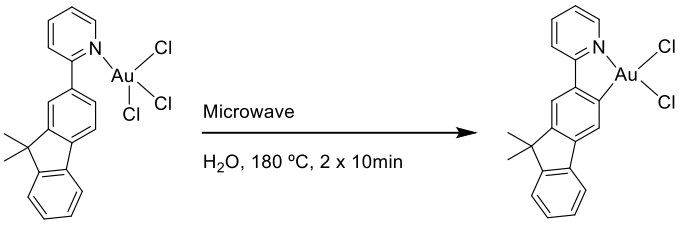


**[fpyAuCl$_3$]** **[fpyAuCl$_2$]**

**[(fpy)$AuCl_3$]** (0.2 g, 0.35 mmol) was suspended in $H_2O$ (12 mL) in a 20 mL microwave vial. Two cycles for 10 min. were made in the microwave at 180 °C. The precipitate was filtered, washed with $H_2O$ and dried *in vacuo* to afford [**(fpy)$AuCl_2$]** (0.1 g, 0.2 mmol, 55%).$^1$H-NMR (400 [MHz], $CDCl_3$, 25 °C): δ [ppm] = 9.83 (*dd*, 1 H, $J_{HH}$ = 4, 0.5, py.), 8.42 (*s*, 1 H, *arom.*), 8.15 – 8.11 (*td*, 1 H, $J_{HH}$ = 8, *arom.*), 7.96 – 7.99 (*dd*, 1 H, $J_{HH}$ = 8, *arom.*), 7.84 – 7.86 (*m*, 1 H, $J_{HH}$ = 8.0, *arom.*), 7.57 (*s*, 1 H, *arom.*), 7.45 – 7.48 (*m*, 2 H, *arom.*), 7.40 – 7.42 (*m*, 2 H, *arom.*), 1.25 (*s*, 6 H, $CH_3$). The NMR data is consistent with the reported literature.

11) [(fpy)AuCl(Fmes)].[91]

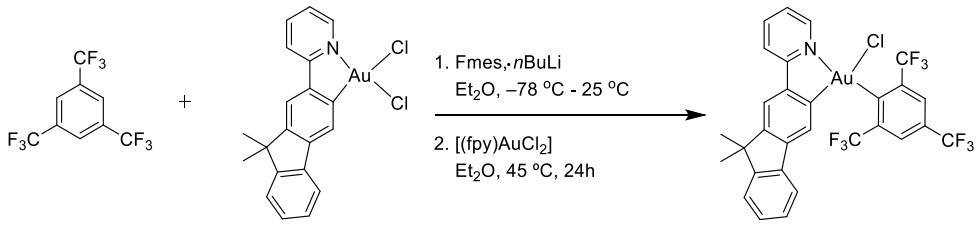


**Fmes** **[(fpy)$AuCl_2$]** **[(fpy)Au(Fmes)Cl]**

1.6 M nBuLi in hexane (1.75mL, 2.8 mmol) was added with the syringe to a Schlenk flask containing Fmes (0.5 mL, 2.5 mmol) in $Et_2O$ (10 mL) and the reaction mixture was stirred for 2h at room temperature. The reaction mixture was transferred to a Young-Schlenk containing suspension of [**(fpy)$AuCl_2$]** (0.2 g, 0.5 mmol) in $Et_2O$ (10 mL). The reaction mixture was heated to 45 °C for 24 h. The mixture was allowed to cool down to room temperature and was then quenched with $H_2O$ (100 mL). The organic layer was extracted with $CH_2Cl_2$ (3 x 30 mL) and washed with brine (100 mL). The combined organic layers were dried over $Na_2SO_4$ and the solvent was removed *in vacuo* to give crude product. The crude product was purified by column chromatography on $SiO_2$ using $CH_2Cl_2$/ Hexane (1:1) and dried under *vacuo to* afford **[fpy)Au(Fmes)Cl]** (0.14 g, 0.18 mmol, 38%) $^1$H-NMR (400 [MHz], $CD_2Cl_2$, 25 °C): δ [ppm] = δ 9.52 (*ddd*, 1 H ,$J_{HH}$ = 5.8, 1.6, 0.7, py.), 8.24 (*s*, 2 H, -*arom.*), 8.19 – 8.12 (*m*, 1 H), 8.08 (*d*, 1 H, $J_{HH}$= 7.9, -*arom.*), 7.78 (*s*, 1 H, -*arom.*), 7.57 (*ddd*, 1 H, $J_{HH}$ = 7.3, 5.8, 1.4, -*arom.*), 7.43 (*d*, 1 H, *J* = 7.5, -*arom.*), 7.36 – 7.29 (*m*, 1 H, -*arom.*), 7.29 – 7.22 (*m*, 2 H, -

*arom.*), 6.60 (*s*, 1 H), 1.51 (s, 6 H, -$CH_3$). $^{13}C\{^1H\}$-NMR (126 [MHz], $CD_2Cl_2$, 25 °C): δ [ppm] = 163.7 (*s*), 154.3 (*s*), 153.1 (*s*), 147.9 (*s*), 142.9 (*s*), 142.1 (*s*), 140.71 (*s*), 137.4 (*s*), 134.6 (*s*), 134.4 (*s*), 128.6 (*s*), 128.6 (*s*), 127.1 (*s*), 124.2 (*s*), 123.7 (*s*), 122.7 (*s*), 120.4 (*s*), 120.2 (*s*), 119.6 (*s*). $^{19}F$ NMR (377 MHz, $CD_2Cl_2$) δ [ppm] = -59.79 (*s*, $CF_3$), -63.19 (*s*, $CF_3$). (+)-HR-ESI-MS (MeOH): calcd for $C_{29}H_{18}AuF_9ClN$ $[M+Na]^+$:*m/z* 806.05418, found 806.05296. Elem. Anal. Calcd for $C_{29}H_{18}AuF_9ClN$ C:44.44, H 2.31, N 1.79. Found, C 45.28, H 2.35, N 1.56.

12) [(bpy)HgCl].[142]

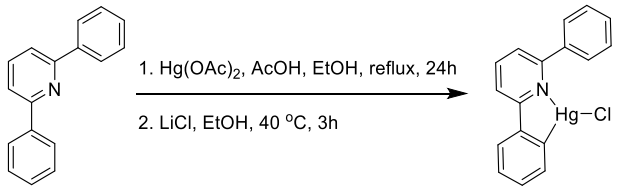


bpy [(bpy)HgCl]

2,6 diphenyl pyridine (0.5 g, 2.2 mmol) and $Hg(OAc)_2$ (0.7 g, 2.2 mmol) were dissolved in 0.2M AcOH in EtOH. The reaction mixture was refluxed for 24 h under nitrogen atmosphere. LiCl (0.6 g, 13.0 mmol) dissolved in EtOH (8 mL) was added to the reaction mixture at 40 °C and stirred for 3 h. The precipitate was filtered and washed with cold EtOH to afford [**(bpy)HgCl]** (2.9 g, 6.2 mmol, 71%) $^1$H-NMR (400 [MHz], DMSO, 25 °C): δ [ppm] = 8.16 (*dd*, 2 H, $J_{HH}$ = 4, 1.4, py.), 8.05 – 7.92 (*m*, 4 H, -*arom.*), 7.68 (*dd*, 1 H, $J_{HH}$ = 1.6, 1.4, -*arom.*), 7.52 – 7.41 (*m*, 5 H, -*arom.*). The NMR data is consistent with the reported literature.

13) [(bpy)AuCl].[143]

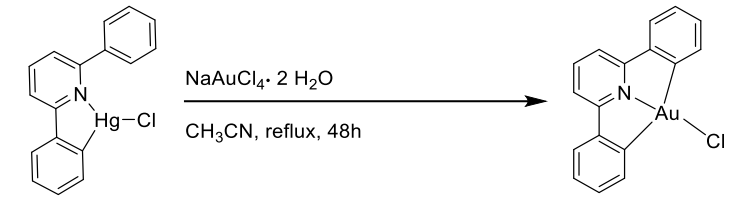


[(bpy)HgCl] [(bpy)AuCl]

Equimolar amounts of **[(bpy)HgCl]** (2.9 g, 6.2 mmol) and $NaAuCl_4.2H_2O$ (2.5 g, 6.2 mmol) were dissolved in $CH_3CN$ (100 mL) and refluxed for 48 h. The reaction mixture was cooled to room temperature, filtered, washed with $CH_3CN$ and $Et_2O$ to deliver **[(bpy)AuCl]** (1.5 g, 3.2 mmol, 52%). $^1$H-NMR (400 [MHz], $CDCl_3$, 25 °C): δ [ppm] = 8.14 (*dd*, 1 H, $J_{HH}$ = 8, -*arom.*), 8.0 (*dd*, 1 H, $J_{HH}$ = 1.1, 1.2, -*arom.*), 7.93 (*dd*, 1 H, $J_{HH}$ = 1.6, 1.4, -*arom.*), 7.61 – 7.57 (*m*, 2 H, -*arom.*), 7.53 – 7.39 (*m*, 5 H, -*arom.*), 7.33 – 7.29 (*m*, 1 H, -*arom.*). The NMR data is consistent with the reported literature.

14) [(bpy)Au(NN)•] [144]

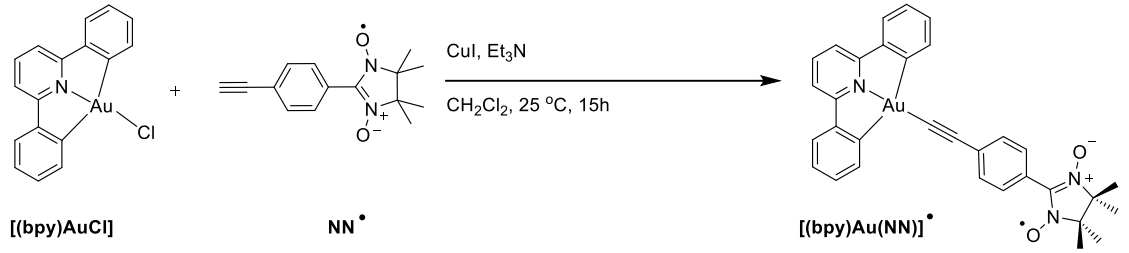


To NN•(50 mg, 0.2 mmol), CuI (80 mg, 0.4 mmol) and $Et_3N$ (40 mg, 0.4 mmol) were added in dry $CH_2Cl_2$ (15 mL). The reaction mixture was stirred overnight at 25 °C. The $CH_2Cl_2$ solution of **[(bpy)AuCl]** (75 mg, 0.16 mmol) was added to the reaction mixture and stirred for 3h. The reaction mixture was quenched with water (30 mL) and extracted with $CH_2Cl_2$ (3 x 30mL). The combined organic layers were dried over $Na_2SO_4$ and the solvent was evaporated. The crude was purified with column chromatography on $Al_2O_3$ using $CH_2Cl_2$/hexane (1:1) as eluent to afford **[(bpy)Au(NN)]•**(28.0 mg, 0.04 mmol, 25%).

**(+)**-HR-ESI-MS (MeOH): calcd for $C_{18}H_{27}AuN_3O_2$• $[M+H]^+$:*m/z* 682.17688, found 682.17553. Elem. Anal. Calcd for $C_{18}H_{27}AuN_3O_2$ C:56.31, H 3.99, N 6.16. Found, C 56.28, H 3.71, N 6.46.

15) [(bpy)AuNN] [138]

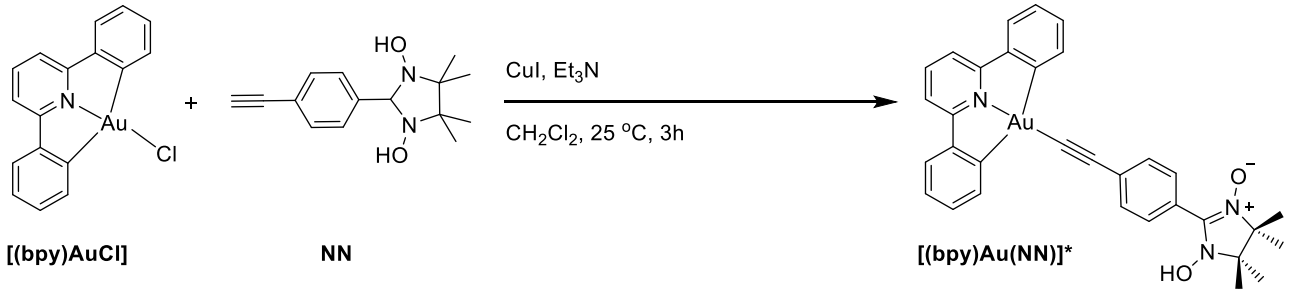


A solution of **[(bpy)AuCl]** (115.0 mg, 0.250 mmol) and CuI (5.0 mg, 0.025 mmol) in dry $CH_2Cl_2$ (15 mL) was treated with $Et_3N$ (1.0 mL, 7.2 mmol). Then **NN (**98 .0 mg, 0.375 mmol**)** was added and the reaction mixture was stirred at 25 °C for 3h. The reaction mixture was quenched with water (30 mL) and extracted with $CH_2Cl_2$ (3 x 30 mL) The combined organic phase was dried over $Na_2SO_4$ and the solvent was evaporated. The crude was purified with column chromatography $CH_2Cl_2$/Hexane (1:1) to afford **[(bpy)AuCl(NN)]*** (12.0 mg, 0.017 mmol, 7%). $^1$H NMR (400 MHz, DMSO) δ [ppm] = 10.03 (*s*, 1H, -OH), 8.19 (*t*, $J_{HH}$ = 8.0, 1H, -*arom*), 8.00 (*d*, $J_{HH}$ = 8.0, 3H, -*arom*), 7.91 (*dd*, *J* = 10.4, 4.2, 8H, -*arom*), 7.73 (*d*, $J_{HH}$ = 8.2, 2H, -*arom*), 7.43 (*td*, $J_{HH}$ = 7.4, 1.3, 2H), 7.34 (*td*, $J_{HH}$ = 7.5, 1.3, 2H, -*arom*), 1.23 (*s*, 12H). (+)-HR-ESI-MS (MeOH): calcd for $C_{32}H_{28}AuN_3O_2$ $[M+H]^+$:*m/z* 684.19255, found 684.19113.

16) [(fpy)Au(Fmes)(NN)]$^{\bullet}$ [145]

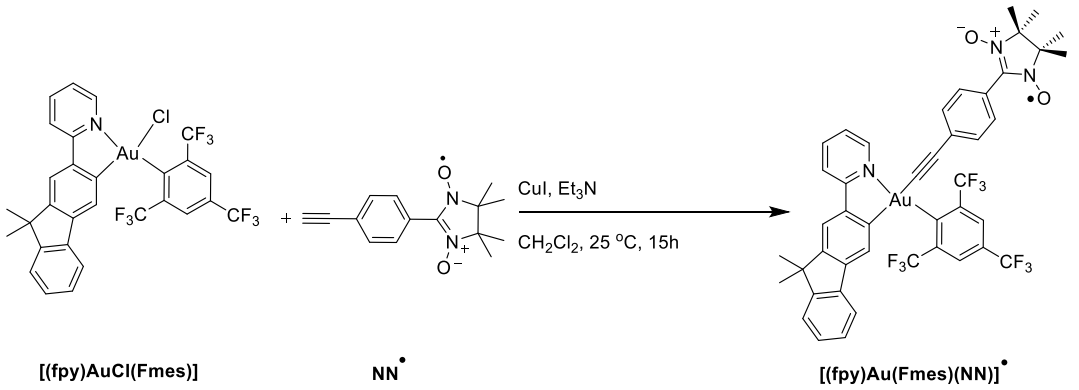


To **NN**$^{\bullet}$ (77 mg, 0.3 mmol), CuI (110 mg, 0.4 mmol) and $Et_3N$ (58 mg, 0.6 mmol) was added in dry $CH_2Cl_2$ (15 mL). The reaction mixture was stirred overnight at 25 °C. The $CH_2Cl_2$ solution of **[(fpy)AuCl(Fmes)]** (150 mg, 0.2 mmol) was added to the reaction mixture and stirred for 3 h. The reaction mixture was quenched with water (30 mL) and extracted with $CH_2Cl_2$ (3 x 30mL). The combined organic layers were dried over $Na_2SO_4$ and the solvent was evaporated. The crude was purified by column chromatography on $Al_2O_3$ using $CH_2Cl_2$/Hexane (1:1) as eluent to afford **[(fpy)Au(Fmes)(NN)$^{\bullet}$]** (50 mg, 0.05 mmol, 25%). (+)-HR-ESI-MS (MeOH): calcd for $C_{44}H_{35}AuF_9N_3O_2^{\bullet}$ $[M+H]^+$:*m/z* 1005.22509, found 1005.22208. Elem. Anal. Calcd for $C_{44}H_{34}AuF_9N_3O_2^{\bullet}$ C:52.60, H 3.41, N 4.18. Found, C 58.46, H 4.46, N 6.22.

17) [(bpy)Pt(DMSO)]. [109]

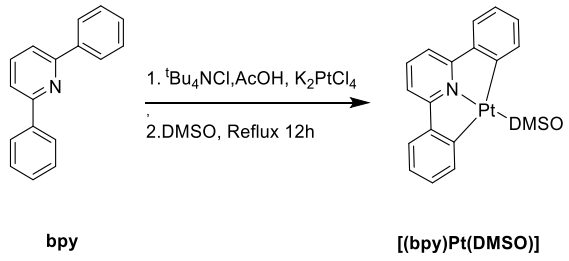


$^t$Bu$_4$NCl (60 mg, 0.2 mmol) and 2,6-biphenyl pyridine (0.43 g, 2.0 mmol) was dissolved in AcOH and degassed for 20 min. Then $K_2PtCl_4$ (0.83 g, 2.0 mmol) was added and the reaction mixture was refluxed for 12 h. The yellow precipitate was filtered off, washed with water and acetone. The yellow solid was dissolved in DMSO (4 mL) and heated to 180-190 °C for 20 min. The solution was poured into water (40 mL), filtered and dissolved in $CH_2Cl_2$ and dried over $Na_2SO_4$. The crude product was purified with column chromatography on $Al_2O_3$ using pure $CH_2Cl_2$ to afford pure **[(bpy)Pt(DMSO)]** (0.41 g, 0.81 mmol, 41%). $^1$H NMR (400 MHz, $CD_2Cl_2$, 25 °C) δ [ppm]= 7.76 (*t*, $J_{HH}$ = 9.6, 1H, -

*arom*), 7.66 (*t*, $J_{HH}$ = 8.0, 1H, -*arom*), 7.49 (*d*, $J_{HH}$ = 7.7 , 1H, -*arom*), 7.37 – 7.31 (*m*, 1H, -*arom*), 7.25 (*ddd*, $J_{HH}$ = 7.4, 4.4, 1.3, 1H, -*arom*), 7.11 (*td*, $J_{HH}$ = 7.6, 1.1, 1H, -*arom*), 3.70 – 3.59 (*m*, 3H, -$CH_3$), 3.70 – 3.59 (*m*, 3H, -$CH_3$). The NMR data is consistent with the reported literature.

18) [(bpy)Pt(α*H*-PyBTM)].[134]

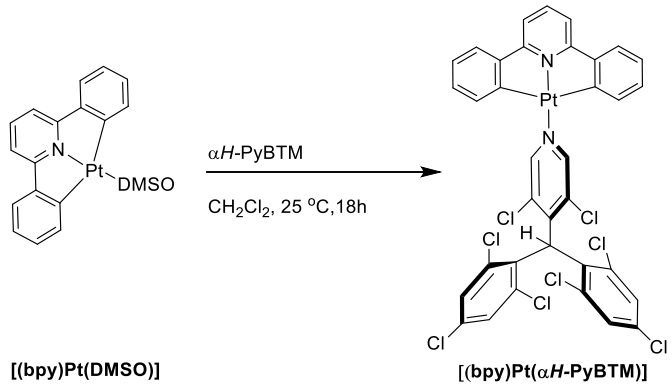


***αH*-PyBTM** (0.255 g, 0.49 mmol) radical was added to the dry $CH_2Cl_2$ solution of **[(bpy)Pt(DMSO)]** (120 mg , 0.24 mmol) and stirred for 18 h. Excess solvent was removed by evaporation and the crude was purified by column chromatography on $SiO_2$ using ($CH_2Cl_2$/Hexane/TEA) (1:1:0.01) as eluent to afford pure **[(bpy)Pt(*αH*-PyBTM)]** (70.0 mg, 0.07 mmol, 31%). $^1$H-NMR (400 MHz, $CD_2Cl_2$, 25 °C): δ [ppm] = 9.09 – 8.91 (*m*, 1H, py), 7.57 (*t*, $J_{HH}$ = 8.0, 1 H, -*arom*), 7.51 – 7.44 (*m*, 2 H, -*arom*), 7.37 (*dd*, $J_{HH}$ = 11.5, 2.2, 1 H, -*arom*), 7.27 (*d*, $J_{HH}$ = 2.9, 1 H, -*arom*), 7.26 (*s*, 1 H, -*arom*), 7.22 (*td*, $J_{HH}$ = 7.3, 1.1, 1 H, -*arom*), 7.07 (*td*, $J_{HH}$ = 7.5, 1.2, 1 H, -*arom*), 6.88 (*dd*, $J_{HH}$ = 7.1, 0.7, 1 H, -*arom*), 6.77 (*s*, 1 H, -CCH). $^{13}$C-NMR (126 MHz, $CD_2Cl_2$): δ [ppm] = 171.9 (*s*), 168.4 (*s*), 152.9 (*s*), 151.3 (*s*), 149.9 (*s*), 149.5 (*s*), 148.2 (*s*), 144.6 (*s*), 140.3 (*s*), 138.2 (*s*), 138.1 (*s*), 137.6 (*s*), 136.9 (*s*), 135.9 (s), 135.1 (*d*, *J* = 8.5), 132.9 (*s*), 132.5 (*s*), 132.4 (*s*), 131.0 (*s*), 130.8 (*s*), 130.5 (*s*), 130.4 (*s*), 129.9 (*s*), 129.1 (*s*), 129.0 (*s*), 128.8 (*s*), 124.3 (*s*), 124.2 (*s*), 114.89 (*s*), 50.29 (*s*).
(+)-HR-ESI-MS (MeOH): calcd for $C_{35}H_{19}PtCl_8N_3$ $[M+H]^+$:*m/z* 941.86989, found 941.86859.
Elem. Anal**.** Calcd for $C_{35}H_{18}PtCl_8N_3$ C:44.47, H 1.92, N 2.96. Found, C 45.46, H 1.99, N 2.92.

19) [(bpy)Pt(PyBTM)]. [134]

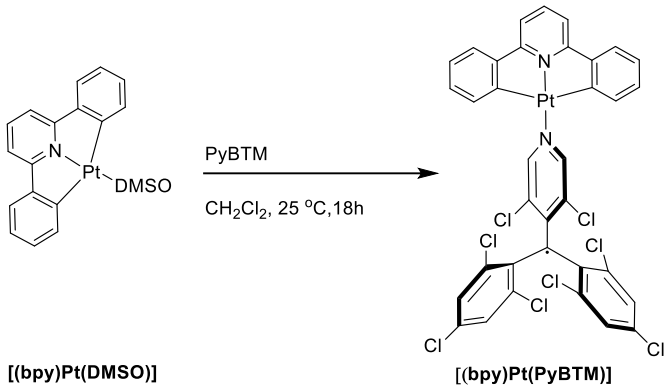


PyBTM (0.4 g, 0.8 mmol) was added to the dry $CH_2Cl_2$ (20 mL) solution of **[(bpy)Pt(DMSO)]** (200 mg, 0.4 mmol) and stirred for 18 h. Excess of solvent was removed by evaporation and the crude was purified by column chromatography on $Al_2O_3$ using (EtOAc/hexane) (1:6) as eluent to deliver **[(bpy)Pt(PyBTM)]** (20 mg, 0.02 mmol, 6%). (+)-HR-ESI-MS (MeOH): calcd for $C_{35}H_{19}Cl_8PtN_2^{\bullet}$ $[M+H]^+$:*m/z* 939.86050, found 939.85820. Elem. Anal**.** Calcd for $C_{35}H_{18}Cl_8PtN_2^{\bullet}$ C:44.52, H 1.81, N 2.97. Found, C 48.52, H 2.81, N 2.64.

# 4 Abbreviations

| | |
|---|---|
| IC | Internal Conversion |
| ISC | Intersystem Crossing |
| SOC | Spin-Orbit Coupling |
| TMSA | Trimethylsilsylacetylene |
| HUMO | Highest Occupied Molecular Orbital |
| LUMO | Lowest Unoccupied Molecular Orbital |
| PMMA | Polymethylmethacrylate |
| PyBTM | 3,5-dichloro-4-pyridyl)bis(2,4,6-trichlorophenyl)methyl radical |
| HRMS | High Resolution Mass Spectrometer |
| EPR | Electron Paramagnetic resonance |
| THF | Tetrahydrofuran |

# 5 References


(1) Anpo, M.; Kondo, M.; Louis, C.; Che, M.; Coluccia, S. Application of Dynamic Photoluminescence Spectroscopy to the Study of the Active Surface Sites on Supported Molybdenum/Silica Catalysts: Features of Anchored and Impregnated Catalysts. *J. Am. Chem. Soc.* **1989**, *111* (24), 8791–8799.

(2) Hattori, Y.; Kusamoto, T.; Nishihara, H. Luminescence, Stability, and Proton Response of an Open-Shell (3,5-Dichloro-4-Pyridyl)Bis(2,4,6-Trichlorophenyl)Methyl Radical. *Angew. Chem. Int. Ed Engl.* **2014**, *53* (44), 11845–11848.

(3) Peng, Q.; Obolda, A.; Zhang, M.; Li, F. Organic Light-Emitting Diodes Using a Neutral π Radical as Emitter: The Emission from a Doublet. *Angew. Chem. Int. Ed.* **2015**, *54* (24), 7091–7095.

(4) Hattori, Y.; Kusamoto, T.; Nishihara, H. Luminescence, Stability, and Proton Response of an Open-Shell (3,5-Dichloro-4-Pyridyl)Bis(2,4,6-Trichlorophenyl)Methyl Radical. *Angew. Chem.* **2014**, *126* (44), 12039–12042.

(5) Hattori, Y.; Kimura, S.; Kusamoto, T.; Maeda, H.; Nishihara, H. Cation-Responsive Turn-on Fluorescence and Absence of Heavy Atom Effects of Pyridyl-Substituted Triarylmethyl Radicals. *Chem. Commun.* **2018**, *54* (6), 615–618.

(6) Hattori, Y.; Kusamoto, T.; Nishihara, H. Enhanced Luminescent Properties of an Open-Shell (3,5-Dichloro-4-Pyridyl)Bis(2,4,6-Trichlorophenyl)Methyl Radical by Coordination to Gold. *Angew. Chem. Int. Ed.* **2015**, *54* (12), 3731–3734.

(7) Kimura, S.; Tanushi, A.; Kusamoto, T.; Kochi, S.; Sato, T.; Nishihara, H. A Luminescent Organic Radical with Two Pyridyl Groups: High Photostability and Dual Stimuli-Responsive Properties, with Theoretical Analyses of Photophysical Processes. *Chem. Sci.* **2018**, *9* (7), 1996–2007..

(8) Ogino, Y.; Kusamoto, T.; Hattori, Y.; Shimada, M.; Tsuchiya, M.; Yamanoi, Y.; Nishibori, E.; Sugimoto, K.; Nishihara, H. Solvent-Controlled Doublet Emission of an Organometallic Gold(I) Complex with a Polychlorinated Diphenyl(4-Pyridyl)Methyl Radical Ligand: Dual Fluorescence and Enhanced Emission Efficiency. *Inorg. Chem.* **2017**, *56* (7), 3909–3915.

(9) Namai, H.; Ikeda, H.; Hoshi, Y.; Kato, N.; Morishita, Y.; Mizuno, K. Thermoluminescence and a New Organic Light-Emitting Diode (OLED) Based on Triplet−Triplet Fluorescence of the Trimethylenemethane (TMM) Biradical. *J. Am. Chem. Soc.* **2007**, *129* (29), 9032–9036.

(10) Obolda, A.; Ai, X.; Zhang, M.; Li, F. Up to 100% Formation Ratio of Doublet Exciton in Deep-Red Organic Light-Emitting Diodes Based on Neutral π-Radical. *ACS Appl. Mater. Interfaces* **2016**, *8* (51), 35472–35478.

(11) Velasco, D.; Castellanos, S.; López, M.; López-Calahorra, F.; Brillas, E.; Juliá, L. Red Organic Light-Emitting Radical Adducts of Carbazole and Tris(2,4,6-Trichlorotriphenyl)Methyl Radical That Exhibit High Thermal Stability and Electrochemical Amphotericity. *J. Org. Chem.* **2007**, *72* (20), 7523–7532.

(12) Colvin, M. T.; Giacobbe, E. M.; Cohen, B.; Miura, T.; Scott, A. M.; Wasielewski, M. R. Competitive Electron Transfer and Enhanced Intersystem Crossing in Photoexcited Covalent TEMPO−Perylene-3,4:9,10-Bis(Dicarboximide) Dyads: Unusual Spin Polarization Resulting from the Radical−Triplet Interaction. *J. Phys. Chem. A* **2010**, *114* (4), 1741–1748.

(13) Mas-Torrent, M.; Crivillers, N.; Mugnaini, V.; Ratera, I.; Rovira, C.; Veciana, J. Organic Radicals on Surfaces: Towards Molecular Spintronics. *J. Mater. Chem.* **2009**, *19* (12), 1691–1695.

(14) Kuppusamy, P.; Chzhan, M.; Vij, K.; Shteynbuk, M.; Lefer, D. J.; Giannella, E.; Zweier, J. L. Three-Dimensional Spectral-Spatial EPR Imaging of Free Radicals in the Heart: A Technique

for Imaging Tissue Metabolism and Oxygenation. *Proc. Natl. Acad. Sci. U. S. A.* **1994**, *91* (8), 3388–3392.
(15) Wang, Y.; Wang, H.; Liu, Y.; Di, C.; Sun, Y.; Wu, W.; Yu, G.; Zhang, D.; Zhu, D. 1-Imino Nitroxide Pyrene for High Performance Organic Field-Effect Transistors with Low Operating Voltage. *J. Am. Chem. Soc.* **2006**, *128* (40), 13058–13059.
(16) Wei, P.; Oh, J. H.; Dong, G.; Bao, Z. Use of a 1H-Benzoimidazole Derivative as an n-Type Dopant and To Enable Air-Stable Solution-Processed n-Channel Organic Thin-Film Transistors. *J. Am. Chem. Soc.* **2010**, *132* (26), 8852–8853.
(17) Pope, M.; Swenberg, C. E. *Electronic Processes in Organic Crystals and Polymers*, Second Edition.; Monographs on the Physics and Chemistry of Materials; Oxford University Press: Oxford, New York, 1999.
(18) Cai, X.; Li, X.; Xie, G.; He, Z.; Gao, K.; Liu, K.; Chen, D.; Cao, Y.; Su, S.-J. "Rate-Limited Effect" of Reverse Intersystem Crossing Process: The Key for Tuning Thermally Activated Delayed Fluorescence Lifetime and Efficiency Roll-off of Organic Light Emitting Diodes. *Chem. Sci.* **2016**, *7* (7), 4264–4275.
(19) Baldo, M. A.; O'Brien, D. F.; You, Y.; Shoustikov, A.; Sibley, S.; Thompson, M. E.; Forrest, S. R. Highly Efficient Phosphorescent Emission from Organic Electroluminescent Devices. *Nature* **1998**, *395*, 151–154.
(20) Ai, X.; Chen, Y.; Feng, Y.; Li, F. A Stable Room-Temperature Luminescent Biphenylmethyl Radical. *Angew. Chem. Int. Ed Engl.* **2018**, *57* (11), 2869–2873.
(21) Heckmann, A.; Dümmler, S.; Pauli, J.; Margraf, M.; Köhler, J.; Stich, D.; Lambert, C.; Fischer, I.; Resch-Genger, U. Highly Fluorescent Open-Shell NIR Dyes: The Time-Dependence of Back Electron Transfer in Triarylamine-Perchlorotriphenylmethyl Radicals. *J. Phys. Chem. C* **2009**, *113* (49), 20958–20966.
(22) Ruberu, S. R.; Fox, M. A. Photochemical Behavior of Stable Free Radicals: The Photochemistry of Perchlorodiphenylmethyl Radical. *J. Phys. Chem.* **1993**, *97* (1), 143–149.
(23) Kimura, S.; Tanushi, A.; Kusamoto, T.; Kochi, S.; Sato, T.; Nishihara, H. A Luminescent Organic Radical with Two Pyridyl Groups: High Photostability and Dual Stimuli-Responsive Properties, with Theoretical Analyses of Photophysical Processes. *Chem. Sci.* **2018**, *9* (7), 1996–2007.
(24) Kusamoto, T.; Kimura, S.; Ogino, Y.; Ohde, C.; Nishihara, H. Modulated Luminescence of a Stable Open-Shell Triarylmethyl Radical: Effects of Chemical Modification on Its Electronic Structure and Physical Properties. *Chem. – Eur. J.* **2016**, *22* (49), 17725–17733.
(25) Hattori, Y.; Kusamoto, T.; Nishihara, H. Highly Photostable Luminescent Open-Shell (3,5-Dihalo-4-Pyridyl)Bis(2,4,6-Trichlorophenyl)Methyl Radicals: Significant Effects of Halogen Atoms on Their Photophysical and Photochemical Properties. *RSC Adv.* **2015**, *5* (79), 64802–64805.
(26) Grilj, J.; Laricheva, E. N.; Olivucci, M.; Vauthey, E. Fluorescence of Radical Ions in Liquid Solution: Wurster's Blue as a Case Study. *Angew. Chem. Int. Ed.* **2011**, *50* (19), 4496–4498.
(27) Hattori, Y.; Kusamoto, T.; Sato, T.; Nishihara, H. Synergistic Luminescence Enhancement of a Pyridyl-Substituted Triarylmethyl Radical Based on Fluorine Substitution and Coordination to Gold. *Chem. Commun.* **2016**, *52* (91), 13393–13396.
(28) Beaulac, R.; Luneau, D.; Reber, C. The Emitting State of the Imino Nitroxide Radical. *Chem. Phys. Lett.* **2005**, *405* (1), 153–158.
(29) Barbieri, A.; Accorsi, G.; Armaroli, N. Luminescent Complexes beyond the Platinum Group : The D10 Avenue. *Chem. Commun.* **2008**, *0* (19), 2185–2193.
(30) Yam, V. W.-W.; Lo, K. K.-W. Luminescent Polynuclear d 10 Metal Complexes. *Chem. Soc. Rev.* **1999**, *28* (5), 323–334.

(31) Wing-Wah Yam, V.; Chung-Chin Cheng, E. Highlights on the Recent Advances in Gold Chemistry—a Photophysical Perspective. *Chem. Soc. Rev.* **2008**, *37* (9), 1806–1813.
(32) Datcu, A.; Roques, N.; Jubera, V.; Maspoch, D.; Fontrodona, X.; Wurst, K.; Imaz, I.; Mouchaham, G.; Sutter, J.-P.; Rovira, C.; et al. Three-Dimensional Porous Metal–Radical Frameworks Based on Triphenylmethyl Radicals. *Chem. – Eur. J.* **2012**, *18* (1), 152–162.
(33) Company, A.; Roques, N.; Güell, M.; Mugnaini, V.; Gómez, L.; Imaz, I.; Datcu, A.; Solà, M.; Luis, J. M.; Veciana, J.; et al. Nanosized Trigonal Prismatic and Antiprismatic CuII Coordination Cages Based on Tricarboxylate Linkers. *Dalton Trans.* **2008**, *0* (13), 1679–1682.
(34) Jinguji, M.; Imamura, T.; Obi, K.; Tanaka, I. Emission Lifetimes of Thiophenoxy Radicals at 77K. *Chem. Phys. Lett.* **1984**, *109* (1), 31–34.
(35) Sakamoto, M.; Cai, X.; Hara, M.; Tojo, S.; Fujitsuka, M.; Majima, T. Anomalous Fluorescence from the Azaxanthone Ketyl Radical in the Excited State. *J. Am. Chem. Soc.* **2005**, *127* (11), 3702–3703.
(36) Kimura, S.; Kusamoto, T.; Kimura, S.; Kato, K.; Teki, Y.; Nishihara, H. Magnetoluminescence in a Photostable, Brightly Luminescent Organic Radical in a Rigid Environment. *Angew. Chem.* **2018**, *130* (39), 12893–12897.
(37) Johnson, R. C.; Merrifield, R. E. Effects of Magnetic Fields on the Mutual Annihilation of Triplet Excitons in Anthracene Crystals. *Phys. Rev. B* **1970**, *1* (2), 896–902.
(38) Merrifield, R. E. Theory of Magnetic Field Effects on the Mutual Annihilation of Triplet Excitons. *J. Chem. Phys.* **1968**, *48* (9), 4318–4319.
(39) Steiner, U. E.; Ulrich, T. Magnetic Field Effects in Chemical Kinetics and Related Phenomena. *Chem. Rev.* **1989**, *89* (1), 51–147.
(40) Mori, Y.; Sakaguchi, Y.; Hayashi, H. Spin Effects on Decay Dynamics of Charge-Separated States Generated by Photoinduced Electron Transfer in Zinc Porphyrin−Naphthalenediimide Dyads. *J. Phys. Chem. A* **2002**, *106* (18), 4453–4467.
(41) Mori, Y.; Sakaguchi, Y.; Hayashi, H. Magnetic Field Effects on the Photoinduced Electron Transfer of 10-Methylphenothiazine with 4-(4-Cyanobenzoyloxy)TEMPO in Fluid Solutions. *Chem. Phys. Lett.* **1998**, *286* (5), 446–451.
(42) Kato, K.; Hagi, S.; Hinoshita, M.; Shikoh, E.; Teki, Y. Photoconductivity and Magnetoconductance Effects on Vacuum Vapor Deposition Films of Weak Charge-Transfer Complexes. *Phys. Chem. Chem. Phys.* **2017**, *19* (29), 18845–18853.
(43) Pan, H.; Shen, Y.; Luan, L.; Lu, K.; Duan, J.; Hu, B. Changing the Sign of Exchange Interaction in Radical Pairs to Tune Magnetic Field Effect on Electrogenerated Chemiluminescence. *J. Phys. Chem. C* **2015**, *119* (15), 8089–8094.
(44) Blasi, D.; Nikolaidou, D. M.; Terenziani, F.; Ratera, I.; Veciana, J. Excimers from Stable and Persistent Supramolecular Radical-Pairs in Red/NIR-Emitting Organic Nanoparticles and Polymeric Films. *Phys. Chem. Chem. Phys.* **2017**, *19* (13), 9313–9319.
(45) Tang, C. W.; VanSlyke, S. A.; Chen, C. H. Electroluminescence of Doped Organic Thin Films. *J. Appl. Phys.* **1989**, *65* (9), 3610–3616.
(46) Kusamoto, T.; Hattori, Y.; Tanushi, A.; Nishihara, H. Intramolecular Ferromagnetic Radical–CuII Coupling in a CuII Complex Ligated with Pyridyl-Substituted Triarylmethyl Radicals. *Inorg. Chem.* **2015**, *54* (9), 4186–4188.
(47) Hattori, Y.; Kusamoto, T.; Sato, T.; Nishihara, H. Synergistic Luminescence Enhancement of a Pyridyl-Substituted Triarylmethyl Radical Based on Fluorine Substitution and Coordination to Gold. *Chem. Commun.* **2016**, *52* (91), 13393–13396.
(48) Ogino, Y.; Kusamoto, T.; Hattori, Y.; Shimada, M.; Tsuchiya, M.; Yamanoi, Y.; Nishibori, E.; Sugimoto, K.; Nishihara, H. Solvent-Controlled Doublet Emission of an Organometallic Gold(I) Complex with a Polychlorinated Diphenyl(4-Pyridyl)Methyl Radical Ligand: Dual Fluorescence and Enhanced Emission Efficiency. *Inorg. Chem.* **2017**, *56* (7), 3909–3915.

(49) Peng, Q.; Obolda, A.; Zhang, M.; Li, F. Organic Light-Emitting Diodes Using a Neutral π Radical as Emitter: The Emission from a Doublet. *Angew. Chem. Int. Ed Engl.* **2015**, *54* (24), 7091–7095.
(50) Francis, T. L.; Mermer, Ö.; Veeraraghavan, G.; Wohlgenannt, M. Large Magnetoresistance at Room Temperature in Semiconducting Polymer Sandwich Devices. *New J. Phys.* **2004**, *6* (1), 185.
(51) Hu, B.; Wu, Y. Tuning Magnetoresistance between Positive and Negative Values in Organic Semiconductors. *Nat. Mater.* **2007**, *6* (12), 985–991.
(52) Chen, P.; Xiong, Z.; Peng, Q.; Bai, J.; Zhang, S.; Li, F. Magneto-Electroluminescence as a Tool to Discern the Origin of Delayed Fluorescence: Reverse Intersystem Crossing or Triplet–Triplet Annihilation? *Adv. Opt. Mater.* **2014**, *2* (2), 142–148.
(53) Nguyen, T. D.; Ehrenfreund, E.; Vardeny, Z. V. Spin-Polarized Light-Emitting Diode Based on an Organic Bipolar Spin Valve. *Science* **2012**, *337* (6091), 204–209.
(54) Peng, Q.; Li, W.; Zhang, S.; Chen, P.; Li, F.; Ma, Y. Evidence of the Reverse Intersystem Crossing in Intra-Molecular Charge-Transfer Fluorescence-Based Organic Light-Emitting Devices Through Magneto-Electroluminescence Measurements. *Adv. Opt. Mater.* **2013**, *1* (5), 362–366.
(55) Thomas, K. R.; Lin, J. T.; Tao, Y. T.; Ko, C. W. Light-Emitting Carbazole Derivatives: Potential Electroluminescent Materials. *J. Am. Chem. Soc.* **2001**, *123* (38), 9404–9411.
(56) Figueira-Duarte, T. M.; Müllen, K. Pyrene-Based Materials for Organic Electronics. *Chem. Rev.* **2011**, *111* (11), 7260–7314.
(57) Lo, M. Y.; Zhen, C.; Lauters, M.; Jabbour, G. E.; Sellinger, A. Organic-Inorganic Hybrids Based on Pyrene Functionalized Octavinylsilsesquioxane Cores for Application in OLEDs. *J. Am. Chem. Soc.* **2007**, *129* (18), 5808–5809.
(58) Chen, W.-C.; Yuan, Y.; Ni, S.-F.; Tong, Q.-X.; Wong, F.-L.; Lee, C.-S. Achieving Efficient Violet-Blue Electroluminescence with CIEy <0.06 and EQE >6% from Naphthyl-Linked Phenanthroimidazole–Carbazole Hybrid Fluorophores. *Chem. Sci.* **2017**, *8* (5), 3599–3608.
(59) Yang, X.; Xu, X.; Zhou, G. Recent Advances of the Emitters for High Performance Deep-Blue Organic Light-Emitting Diodes. *J. Mater. Chem. C* **2015**, *3* (5), 913–944.
(60) Beldjoudi, Y.; Nascimento, M. A.; Cho, Y. J.; Yu, H.; Aziz, H.; Tonouchi, D.; Eguchi, K.; Matsushita, M. M.; Awaga, K.; Osorio-Roman, I.; et al. Multifunctional Dithiadiazolyl Radicals: Fluorescence, Electroluminescence, and Photoconducting Behavior in Pyren-1'-Yl-Dithiadiazolyl. *J. Am. Chem. Soc.* **2018**, *140* (20), 6260–6270.
(61) Fairhurst, S. A.; Johnson, K. M.; Sutcliffe, L. H.; Preston, K. F.; Banister, A. J.; Hauptman, Z. V.; Passmore, J. Electron Spin Resonance Study of CH3CNSSN˙, C6H5CNSSN˙, and SNSSN˙+ Free Radicals. *J. Chem. Soc. Dalton Trans.* **1986**, *0* (7), 1465–1472.
(62) Brooks, W. V. F.; Burford, N.; Passmore, J.; Schriver, M. J.; Sutcliffe, L. H. Paramagnetic Liquids: The Preparation and Characterisation of the Thermally Stable Radical ButCNSNS· and Its Quantitative Photochemically Symmetry Allowed Rearrangement to a Second Stable Radical ButCNSSN. *J. Chem. Soc. Chem. Commun.* **1987**, *0* (2), 69–71.
(63) Britten, J.; Hearns, N. G. R.; Preuss, K. E.; Richardson, J. F.; Bin-Salamon, S. Mn(II) and Cu(II) Complexes of a Dithiadiazolyl Radical Ligand: Monomer/Dimer Equilibria in Solution. *Inorg. Chem.* **2007**, *46* (10), 3934–3945.
(64) Green, S. A.; Simpson, D. J.; Zhou, G.; Ho, P. S.; Blough, N. V. Intramolecular Quenching of Excited Singlet States by Stable Nitroxyl Radicals. *J. Am. Chem. Soc.* **1990**, *112* (20), 7337–7346.
(65) Laferrière, M.; Galian, R. E.; Maurel, V.; Scaiano, J. C. Non-Linear Effects in the Quenching of Fluorescent Quantum Dots by Nitroxyl Free Radicals. *Chem. Commun.* **2006**, *0* (3), 257–259.

(66) Blinco, J. P.; Fairfull-Smith, K. E.; Morrow, B. J.; Bottle, S. E. Profluorescent Nitroxides as Sensitive Probes of Oxidative Change and Free Radical Reactions†. *Aust. J. Chem.* **2011**, *64* (4), 373–389.
(67) Lin, F.; Pei, D.; He, W.; Huang, Z.; Huang, Y.; Guo, X. Electron Transfer Quenching by Nitroxide Radicals of the Fluorescence of Carbon Dots. *J. Mater. Chem.* **2012**, *22* (23), 11801–11807.
(68) Rajca, A.; Olankitwanit, A.; Rajca, S. Triplet Ground State Derivative of Aza-m-Xylylene Diradical with Large Singlet−Triplet Energy Gap. *J. Am. Chem. Soc.* **2011**, *133* (13), 4750–4753.
(69) Hiraoka, S.; Okamoto, T.; Kozaki, M.; Shiomi, D.; Sato, K.; Takui, T.; Okada, K. A Stable Radical-Substituted Radical Cation with Strongly Ferromagnetic Interaction: Nitronyl Nitroxide-Substituted 5,10-Diphenyl-5,10-Dihydrophenazine Radical Cation. *J. Am. Chem. Soc.* **2004**, *126* (1), 58–59.
(70) Suzuki, S.; Wada, T.; Tanimoto, R.; Kozaki, M.; Shiomi, D.; Sugisaki, K.; Sato, K.; Takui, T.; Miyake, Y.; Hosokoshi, Y.; et al. Cyclic Triradicals Composed of Iminonitroxide–Gold(I) with Intramolecular Ferromagnetic Interactions. *Angew. Chem. Int. Ed.* **2016**, *55* (36), 10791–10794.
(71) Haase, W. Oliver Kahn: Molecular Magnetism. VCH-Verlag, Weinheim, New York 1993. ISBN 3-527-89566-3, 380 Seiten, Preis: DM 154,—. *Berichte Bunsenges. Für Phys. Chem.* **1994**, *98* (9), 1208–1208.
(72) *Molecular Nanomagnets*; Mesoscopic Physics and Nanotechnology; Oxford University Press: Oxford, New York, 2006.
(73) Pal, S. K.; Itkis, M. E.; Tham, F. S.; Reed, R. W.; Oakley, R. T.; Haddon, R. C. Resonating Valence-Bond Ground State in a Phenalenyl-Based Neutral Radical Conductor. *Science* **2005**, *309* (5732), 281–284.
(74) Iwasaki, A.; Hu, L.; Suizu, R.; Nomura, K.; Yoshikawa, H.; Awaga, K.; Noda, Y.; Kanai, K.; Ouchi, Y.; Seki, K.; et al. Interactive Radical Dimers in Photoconductive Organic Thin Films. *Angew. Chem. Int. Ed Engl.* **2009**, *48* (22), 4022–4024.
(75) Johan Ullman Inventions, Patents and Patent Applications - Justia Patents Search https://patents.justia.com/inventor/johan-ullman (accessed Apr 18, 2019).
(76) Vezzu, D. A. K.; Deaton, J. C.; Jones, J. S.; Bartolotti, L.; Harris, C. F.; Marchetti, A. P.; Kondakova, M.; Pike, R. D.; Huo, S. Highly Luminescent Tetradentate Bis-Cyclometalated Platinum Complexes: Design, Synthesis, Structure, Photophysics, and Electroluminescence Application. *Inorg. Chem.* **2010**, *49* (11), 5107–5119.
(77) Company, A.; Roques, N.; Güell, M.; Mugnaini, V.; Gómez, L.; Imaz, I.; Datcu, A.; Solà, M.; Luis, J. M.; Veciana, J.; et al. Nanosized Trigonal Prismatic and Antiprismatic CuII Coordination Cages Based on Tricarboxylate Linkers. *Dalton Trans.* **2008**, *0* (13), 1679–1682.
(78) Datcu, A.; Roques, N.; Jubera, V.; Maspoch, D.; Fontrodona, X.; Wurst, K.; Imaz, I.; Mouchaham, G.; Sutter, J.-P.; Rovira, C.; et al. Three-Dimensional Porous Metal–Radical Frameworks Based on Triphenylmethyl Radicals. *Chem. – Eur. J.* **2012**, *18* (1), 152–162.
(79) Zhang, X.; Suzuki, S.; Kozaki, M.; Okada, K. NCN Pincer–Pt Complexes Coordinated by (Nitronyl Nitroxide)-2-Ide Radical Anion. *J. Am. Chem. Soc.* **2012**, *134* (43), 17866–17868. https://doi.org/10.1021/ja308103g.
(80) Arx, T. von; Szentkuti, A.; Zehnder, T. N.; Blacque, O.; Venkatesan, K. Stable N-Heterocyclic Carbene (NHC) Cyclometalated (C^C) Gold(III) Complexes as Blue–Blue Green Phosphorescence Emitters. *J. Mater. Chem. C* **2017**, *5* (15), 3765–3769.
(81) Roşca, D.-A.; Smith, D. A.; Bochmann, M. Cyclometallated Gold(III) Hydroxides as Versatile Synthons for Au–N, Au–C Complexes and Luminescent Compounds. *Chem. Commun.* **2012**, *48* (58), 7247–7249.

(82) Pernpointner, M.; Hashmi, A. S. K. Fully Relativistic, Comparative Investigation of Gold and Platinum Alkyne Complexes of Relevance for the Catalysis of Nucleophilic Additions to Alkynes. *J. Chem. Theory Comput.* **2009**, *5* (10), 2717–2725.
(83) Dequirez, G.; Pons, V.; Dauban, P. Nitrene Chemistry in Organic Synthesis: Still in Its Infancy? *Angew. Chem. Int. Ed Engl.* **2012**, *51* (30), 7384–7395.
(84) Gramage-Doria, R.; Reek, J. N. H. New Endeavors in Gold Catalysis—Size Matters. *Angew. Chem. Int. Ed.* **2013**, *52* (50), 13146–13148.
(85) Xiao, J.; Li, X. Gold α-Oxo Carbenoids in Catalysis: Catalytic Oxygen-Atom Transfer to Alkynes. *Angew. Chem. Int. Ed Engl.* **2011**, *50* (32), 7226–7236.
(86) Gorin, D. J.; Toste, F. D. Relativistic Effects in Homogeneous Gold Catalysis. *Nature* **2007**, *446* (7134), 395–403.
(87) Fürstner, A.; Davies, P. W. Catalytic Carbophilic Activation: Catalysis by Platinum and Gold Pi Acids. *Angew. Chem. Int. Ed Engl.* **2007**, *46* (19), 3410–3449.
(88) Dorel, R.; Echavarren, A. M. Gold(I)-Catalyzed Activation of Alkynes for the Construction of Molecular Complexity. *Chem. Rev.* **2015**, *115* (17), 9028–9072.
(89) Kumar, R.; Nevado, C. Cyclometalated Gold(III) Complexes: Synthesis, Reactivity, and Physicochemical Properties. *Angew. Chem. Int. Ed.* **2017**, *56* (8), 1994–2015.
(90) Bachmann, M.; Fessler, R.; Blacque, O.; Venkatesan, K. Towards Blue Emitting Monocyclometalated Gold(III) Complexes – Synthesis, Characterization and Photophysical Investigations. *Dalton Trans.* **2019**.
(91) Szentkuti, A.; Bachmann, M.; Garg, J. A.; Blacque, O.; Venkatesan, K. Monocyclometalated Gold(III) Monoaryl Complexes—A New Class of Triplet Phosphors with Highly Tunable and Efficient Emission Properties. *Chem. – Eur. J.* **2014**, *20* (9), 2585–2596.
(92) Garg, J. A.; Blacque, O.; Venkatesan, K. Syntheses and Photophysical Properties of Luminescent Mono-Cyclometalated Gold(III) Cis-Dialkynyl Complexes. *Inorg. Chem.* **2011**, *50* (12), 5430–5441.
(93) Szentkuti, A.; Garg, J. A.; Blacque, O.; Venkatesan, K. Monocyclometalated Gold(III) Complexes Bearing π-Accepting Cyanide Ligands: Syntheses, Structural, Photophysical, and Electrochemical Investigations. *Inorg. Chem.* **2015**, *54* (22), 10748–10760.
(94) Garg, J. A.; Blacque, O.; Fox, T.; Venkatesan, K. Stable and Tunable Phosphorescent Neutral Cyclometalated Au(III) Diaryl Complexes. *Inorg. Chem.* **2010**, *49* (24), 11463–11472.
(95) *Molecular Organometallic Materials for Optics*; Bozec, H., Guerchais, V., Eds.; Topics in Organometallic Chemistry; Springer-Verlag: Berlin Heidelberg, 2010.
(96) *Photochemistry and Photophysics of Coordination Compounds II*; Balzani, V., Campagna, S., Eds.; Topics in Current Chemistry, Photochemistry and Photophysics of Coordination Compounds; Springer-Verlag: Berlin Heidelberg, 2007.
(97) Williams, J. A. G. The Coordination Chemistry of Dipyridylbenzene: N-Deficient Terpyridine or Panacea for Brightly Luminescent Metal Complexes? *Chem. Soc. Rev.* **2009**, *38* (6), 1783–1801.
(98) Tseng, C.-H.; Fox, M. A.; Liao, J.-L.; Ku, C.-H.; Sie, Z.-T.; Chang, C.-H.; Wang, J.-Y.; Chen, Z.-N.; Lee, G.-H.; Chi, Y. Luminescent Pt(II) Complexes Featuring Imidazolylidene–Pyridylidene and Dianionic Bipyrazolate: From Fundamentals to OLED Fabrications. *J. Mater. Chem. C* **2017**, *5* (6), 1420–1435.
(99) Chi, Y.; Chou, P.-T. Transition-Metal Phosphors with Cyclometalating Ligands: Fundamentals and Applications. *Chem. Soc. Rev.* **2010**, *39* (2), 638–655.
(100) Thomas, S. W.; Venkatesan, K.; Müller, P.; Swager, T. M. Dark-Field Oxidative Addition-Based Chemosensing: New Bis-Cyclometalated Pt(II) Complexes and Phosphorescent Detection of Cyanogen Halides. *J. Am. Chem. Soc.* **2006**, *128* (51), 16641–16648.

(101) Iii, S. W. T.; Yagi, S.; Swager, T. M. Towards Chemosensing Phosphorescent Conjugated Polymers: Cyclometalated Platinum(II) Poly(Phenylene)s. *J. Mater. Chem.* **2005**, *15* (27–28), 2829–2835.
(102) Chan, J. C.-H.; Lam, W. H.; Wong, H.-L.; Zhu, N.; Wong, W.-T.; Yam, V. W.-W. Diarylethene-Containing Cyclometalated Platinum(II) Complexes: Tunable Photochromism via Metal Coordination and Rational Ligand Design. *J. Am. Chem. Soc.* **2011**, *133* (32), 12690–12705.
(103) Huang, Z.; Liu, B.; Zhao, J.; He, Y.; Yan, X.; Xu, X.; Zhou, G.; Yang, X.; Wu, Z. Platinum(II) Polymetallayne-Based Phosphorescent Polymers with Enhanced Triplet Energy-Transfer: Synthesis, Photophysical, Electrochemistry, and Electrophosphorescent Investigation. *RSC Adv.* **2015**, *5* (46), 36507–36519.
(104) Brooks, J.; Babayan, Y.; Lamansky, S.; Djurovich, P. I.; Tsyba, I.; Bau, R.; Thompson, M. E. Synthesis and Characterization of Phosphorescent Cyclometalated Platinum Complexes. *Inorg. Chem.* **2002**, *41* (12), 3055–3066.
(105) Rao, Y.-L.; Wang, S. Impact of Cyclometalation and π-Conjugation on Photoisomerization of an N,C-Chelate Organoboron Compound. *Organometallics* **2011**, *30* (16), 4453–4458.
(106) Tam, A. Y.-Y.; Tsang, D. P.-K.; Chan, M.-Y.; Zhu, N.; Yam, V. W.-W. A Luminescent Cyclometalated Platinum(II) Complex and Its Green Organic Light Emitting Device with High Device Performance. *Chem. Commun.* **2011**, *47* (12), 3383–3385.
(107) Yam, V. W.-W.; Choi, S. W.-K.; Lai, T.-F.; Lee, W.-K. Syntheses, Crystal Structures and Photophysics of Organogold(III) Diimine Complexes. *J. Chem. Soc. Dalton Trans.* **1993**, *0* (6), 1001–1002.
(108) Moussa, J.; Loch, A.; Chamoreau, L.-M.; Degli Esposti, A.; Bandini, E.; Barbieri, A.; Amouri, H. Luminescent Cyclometalated Platinum Complexes with π-Bonded Catecholate Organometallic Ligands. *Inorg. Chem.* **2017**, *56* (4), 2050–2059.
(109) Kulikova, M. V.; Balashev, K. P.; Erzin, Kh. Synthesis and Photophysical Properties of a Series of Biscyclometalated Platinum(II) Complexes on the Basis of a Tridentate 2,6-Diphenylpyridine. *Russ. J. Gen. Chem.* **2003**, *73* (12), 1839–1845.
(110) Bachmann, M.; Blacque, O.; Venkatesan, K. Stable and Color Tunable Emission Properties Based on Non-Cyclometalated Gold(III) Complexes. *Dalton Trans.* **2015**, *44* (21), 10003–10013.
(111) Kumar, R.; Linden, A.; Nevado, C. Luminescent (N^C^C) Gold(III) Complexes: Stabilized Gold(III) Fluorides. *Angew. Chem. Int. Ed.* **2015**, *54* (48), 14287–14290.
(112) Lee, C.-H.; Tang, M.-C.; Cheung, W.-L.; Lai, S.-L.; Chan, M.-Y.; Yam, V. W.-W. Highly Luminescent Phosphine Oxide-Containing Bipolar Alkynylgold(Iii) Complexes for Solution-Processable Organic Light-Emitting Devices with Small Efficiency Roll-Offs †Electronic Supplementary Information (ESI) Available. See DOI: 10.1039/C8sc02265h. *Chem. Sci.* **2018**, *9* (29), 6228–6232.
(113) Zhang, X.; Wright, A. M.; DeYonker, N. J.; Hollis, T. K.; Hammer, N. I.; Webster, C. E.; Valente, E. J. Synthesis, Air Stability, Photobleaching, and DFT Modeling of Blue Light Emitting Platinum CCC-N-Heterocyclic Carbene Pincer Complexes. *Organometallics* **2012**, *31* (5), 1664–1672.
(114) Yam, V. W.-W.; Li, C.-K.; Chan, C.-L.; Cheung, K.-K. Synthesis, Structural Characterization, and Photophysics of Dinuclear Gold(II) Complexes [{Au(Dppn)Br}2](PF6)2 and [{Au(Dppn)I}2](PF6)2 with an Unsupported AuII−AuII Bond. *Inorg. Chem.* **2001**, *40* (27), 7054–7058.
(115) Tang, M.-C.; Tsang, D. P.-K.; Chan, M. M.-Y.; Wong, K. M.-C.; Yam, V. W.-W. Dendritic Luminescent Gold(III) Complexes for Highly Efficient Solution-Processable Organic Light-Emitting Devices. *Angew. Chem. Int. Ed.* **2013**, *52* (1), 446–449.

(116) Lu, W.; Chan, K. T.; Wu, S.-X.; Chen, Y.; Che, C.-M. Quest for an Intermolecular Au(III)···Au(III) Interaction between Cyclometalated Gold(III) Cations. *Chem. Sci.* **2012**, *3* (3), 752–755.
(117) Wong, K. H.; Cheung, K. K.; Chan, M. C. W.; Che, C. M. Application of 2,6-Diphenylpyridine as a Tridentate [C∧N∧C] Dianionic Ligand in Organogold(III) Chemistry. Structural and Spectroscopic Properties of Mono- and Binuclear Transmetalated Gold(III) Complexes. **1998**.
(118) To, W.-P.; Chan, K. T.; Tong, G. S. M.; Ma, C.; Kwok, W.-M.; Guan, X.; Low, K.-H.; Che, C.-M. Strongly Luminescent Gold(III) Complexes with Long-Lived Excited States: High Emission Quantum Yields, Energy Up-Conversion, and Nonlinear Optical Properties. *Angew. Chem. Int. Ed.* **2013**, *52* (26), 6648–6652.
(119) Zhang, P.; Chiu, C. K. C.; Huang, H.; Lam, Y. P. Y.; Habtemariam, A.; Malcomson, T.; Paterson, M. J.; Clarkson, G. J.; O'Connor, P. B.; Chao, H.; et al. Organoiridium Photosensitizers Induce Specific Oxidative Attack on Proteins within Cancer Cells. *Angew. Chem.* **2017**, *129* (47), 15094–15098.
(120) Wautelet, P.; Le Moigne, J.; Videva, V.; Turek, P. Spin Exchange Interaction through Phenylene-Ethynylene Bridge in Diradicals Based on Iminonitroxide and Nitronylnitroxide Radical Derivatives. 1. Experimental Investigation of the Through-Bond Spin Exchange Coupling. *J. Org. Chem.* **2003**, *68* (21), 8025–8036.
(121) Klyatskaya, S. V.; Tretyakov, E. V.; Vasilevsky, S. F. Cross-Coupling of Aryl Iodides with Paramagnetic Terminal Acetylenes Derived from 4,4,5,5-Tetramethyl-2-Imidazoline-1-Oxyl 3-Oxide. *Russ. Chem. Bull.* **2002**, *51* (1), 128–134.
(122) B. Borozdina, Y.; Mostovich, E.; Enkelmann, V.; Wolf, B.; T. Cong, P.; Tutsch, U.; Lang, M.; Baumgarten, M. Interacting Networks of Purely Organic Spin–1/2 Dimers. *J. Mater. Chem. C* **2014**, *2* (32), 6618–6629.
(123) Hattori, Y.; Kusamoto, T.; Nishihara, H. Luminescence, Stability, and Proton Response of an Open-Shell (3,5-Dichloro-4-Pyridyl)Bis(2,4,6-Trichlorophenyl)Methyl Radical. *Angew. Chem. Int. Ed Engl.* **2014**, *53* (44), 11845–11848.
(124) Rendy; Zhang, Y.; McElrea, A.; Gomez, A.; Klumpp, D. A. Superacid-Catalyzed Reactions of Cinnamic Acids and the Role of Superelectrophiles1. *J. Org. Chem.* **2004**, *69* (7), 2340–2347.
(125) Rasul, G.; Olah, G. A. Calculational Study of the Protonation of BXH 2 and BX 2 H (X = F and Cl). Structures of BXH 3 + and BX 2 H 2 + and Their Dihydrogen Complexes BXH 5 + and BX 2 H 4 + 1. *Inorg. Chem. 40* (10), 2453–2456.
(126) Klumpp, D. A.; Zhang, Y.; Kindelin, P. J.; Lau, S. Superacid-Catalyzed Reactions of Pyridinecarboxaldehydes. *Tetrahedron* **2006**, *62* (25), 5915–5921.
(127) Superacid-catalyzed reactions of pyridinecarboxaldehydes - ScienceDirect https://www.sciencedirect.com/science/article/pii/S0040402006006193 (accessed Apr 18, 2019).
(128) Klumpp, D. A.; Garza, M.; Jones, A.; Mendoza, S. Synthesis of Aryl-Substituted Piperidines by Superacid Activation of Piperidones. *J. Org. Chem.* **1999**, *64* (18), 6702–6705.
(129) Yam, V. W.-W.; Wong, K. M.-C.; Hung, L.-L.; Zhu, N. Luminescent Gold(III) Alkynyl Complexes: Synthesis, Structural Characterization, and Luminescence Properties. *Angew. Chem. Int. Ed Engl.* **2005**, *44* (20), 3107–3110. https://doi.org/10.1002/anie.200500253.
(130) Wong, K. M. C.; Zhu, X.; Hung, L. L.; Zhu, N.; Yam, V. W. W.; Kwok, H. S. A Novel Class of Phosphorescent Gold(III) Alkynyl-Based Organic Light-Emitting Devices with Tunable Colour. **2005**.
(131) Johnson, M. W.; DiPasquale, A. G.; Bergman, R. G.; Toste, F. D. Synthesis of Stable Gold(III) Pincer Complexes with Anionic Heteroatom Donors. *Organometallics* **2014**, *33* (16), 4169–4172.

(132) Yam, V. W.-W.; Wong, K. M.-C. Luminescent Metal Complexes of D6, D8 and D10 Transition Metal Centres. *Chem. Commun.* **2011**, *47* (42), 11579–11592.
(133) Hung, L.-L.; Lam, W. H.; Wong, K. M.-C.; Cheng, E. C.-C.; Zhu, N.; Yam, V. W.-W. Synthesis, Luminescence and Electrochemical Properties of Luminescent Dinuclear Mixed-Valence Gold Complexes with Alkynyl Bridges. *Inorg. Chem. Front.* **2015**, *2* (5), 453–466.
(134) Sooksawat, D.; J. Pike, S.; Z. Slawin, A. M.; J. Lusby, P. Acid–Base Responsive Switching between "3+1" and "2+2" Platinum Complexes. *Chem. Commun.* **2013**, *49* (94), 11077–11079.
(135) Bachmann, M.; Blacque, O.; Venkatesan, K. Harnessing White-Light Luminescence via Tunable Singlet-and Triplet-Derived Emissions Based on Gold(III) Complexes *. *Chem. – Eur. J.* **2017**, *23* (40), 9451–9456.
(136) Ullman, E. F.; Osiecki, J. H.; Boocock, D. G. B.; Darcy, R. Stable Free Radicals. X. Nitronyl Nitroxide Monoradicals and Biradicals as Possible Small Molecule Spin Labels. *J. Am. Chem. Soc.* **1972**, *94* (20), 7049–7059.
(137) Room-Temperature Electron Spin Relaxation of Triarylmethyl Radicals at the X- and Q-Bands https://pubs.acs.org/doi/pdf/10.1021/acs.jpcb.5b03027 (accessed Apr 18, 2019).
(138) Au, V. K.-M.; Zhu, N.; Yam, V. W.-W. Luminescent Metallogels of Bis-Cyclometalated Alkynylgold(III) Complexes. *Inorg. Chem.* **2013**, *52* (2), 558–567.
(139) Tsuboyama, A.; Iwawaki, H.; Furugori, M.; Mukaide, T.; Kamatani, J.; Igawa, S.; Moriyama, T.; Miura, S.; Takiguchi, T.; Okada, S.; et al. Homoleptic Cyclometalated Iridium Complexes with Highly Efficient Red Phosphorescence and Application to Organic Light-Emitting Diode. *J. Am. Chem. Soc.* **2003**, *125* (42), 12971–12979. https://doi.org/10.1021/ja034732d.
(140) Organic Mechanisms: Reactions, Stereochemistry and Synthesis. *Choice Rev. Online* **2010**, *48* (03), 48-1479-48–1479.
(141) Bachmann, M.; Fessler, R.; Blacque, O.; Venkatesan, K. Towards Blue Emitting Monocyclometalated Gold( Iii ) Complexes – Synthesis, Characterization and Photophysical Investigations. *Dalton Trans.* **2019**.
(142) Bronner, C.; Wenger, O. S. Luminescent Cyclometalated Gold(III) Complexes. *Dalton Trans.* **2011**, *40* (46), 12409–12420.
(143) Grisorio, R.; Suranna, G. P.; Mastrorilli, P.; Mazzeo, M.; Colella, S.; Carallo, S.; Gigli, G. Aryl 5-Substitution of a Phenyl-Pyridine Based Ligand as a Viable Way to Influence the Opto-Electronic Properties of Bis-Cyclometalated Ir(III) Heteroleptic Complexes. *Dalton Trans.* **2013**, *42* (24), 8939–8950.
(144) Nast, R. Coordination Chemistry of Metal Alkynyl Compounds. *Coord. Chem. Rev.* **1982**, *47* (1), 89–124.
(145) Theunissen, C.; Lecomte, M.; Jouvin, K.; Laouiti, A.; Guissart, C.; Heimburger, J.; Loire, E.; Evano, G. Convenient and Practical Alkynylation of Heteronucleophiles with Copper Acetylides. *Synthesis* **2014**, *46* (9), 1157–1166.